Eidgenössische Technische Hochschule Zürich
Swiss Federal Institute of Technology Zurich

Study of the interaction of *S.* Typhimurium effector protein SopE with *Salmonella*-containing vacuoles

Master thesis of Steven Cardini

12th March 2012

Referee: Prof. Dr. Wolf-Dietrich Hardt

Co-referee: Prof. Dr. Annette Oxenius

Supervisor: Pascale Vonaesch

Institute of Microbiology, ETH Zurich

Group of Prof. Dr. Wolf-Dietrich Hardt

Abstract

The *S*. Typhimurium effector protein SopE is a Guanine nucleotide exchange factor and promotes invasion into host cells by inducing membrane ruffling. It has been found to associate with *Salmonella*-containing vacuoles (SCVs) *in vitro*. In this study diverse approaches were taken to investigate whether phosphorylation, ubiquitination or prenylation by GGTase-I is required for the localization of SopE to SCVs. Furthermore, we tested if the effector has the potential to directly bind to lipids of the SCVs. Phosphorylation, ubiquitination and GGTase-I prenylation were found to be dispensable for the localization of SopE to SCVs and no direct binding of secreted SopE to lipids was detected.

Additionally we found that the treatment of cells with the bacterial translation inhibitor chloramphenicol lead to abolishment of SopE localization to SCVs. The results of this study suggest that SopE is continuously translocated after cell invasion and propose a secondary role for the effector protein at later stages of infections.

Contents

1. Introduction

1.1. The gut microbiota and salmonellosis

Microorganisms of many different species live in close symbiosis with vertebrates. In *Homo sapiens* the highest density is found in the colon with up to 10^{12} bacteria per gram of feces [8]. This gut microbiota is thought to be composed of more than 1000 different bacterial species, most of which belong to only four bacterial phyla, and some fungal and protist species [9]. Co-existence in this environment is finely tuned to a relatively stable equilibrium and has evolved to support resistance to gut colonization by exogenous microorganisms through various mechanisms [10]. Yet, in spite of this "colonization resistance" [10] introduced by the microbiota and host defenses such as the natural barrier function of the mucosa and the immune system, a large proportion of bacterial infections still originate in the intestine. Pathogenic bacteria have evolved diverse means to overcome these obstacles and cause an infection in humans.

The genus of Gram-negative, rod-shaped *Salmonella* belongs to the family *Enterobacteriaceae* and has diverged from the lineage of *Escherichia coli* roughly 100 million years ago [11]. At present the genus is divided into two species, namely *Salmonella bongori* and *Salmonella enterica* (see Fig. 1.1). The latter contains several subspecies and some of them can cause a variety of diseases in humans, including systemic (typhoid) fevers or acute gastroenteritis [12]. *S. enterica* subspecies I serovar Typhimurium (here referred to as *S*. Typhimurium or *S*. Tm) is one of these bacteria. The facultative intracellular pathogen has evolved means to induce

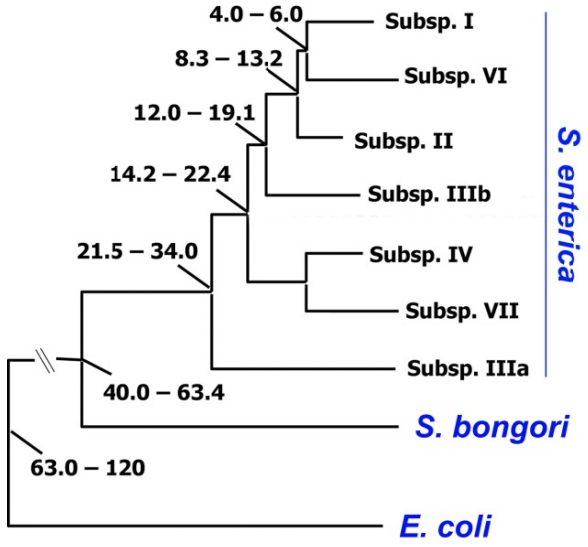

Fig. 1.1 | Phylogenetic tree showing the lineage of *Salmonella* species. Numbers represent common ancestors in millions of years ago [6].

gastroenteritis in healthy humans and thereby perturb the physiological microbiota. *S.* Typhimurium is most commonly taken up orally via contaminated food or water and frequently elicits nausea, diarrhea and vomiting with an incubation period of six to twelve hours [13]. In more severe cases symptoms may include abdominal cramps and fever [13]. Still today salmonellosis is a high burden to humanity as every year more than 90 million humans develop gastroenteritis due to nontyphoidal *Salmonella* infections and roughly 150.000 die as a result of illness [13].

1.2. Type III secretion systems in general and in *Salmonella*

Invasive bacteria are equipped with a wide variety of different virulence factors that enable them to colonize their hosts. Type III secretion systems (TTSS) are examples of very potent virulence factors and are encoded by several pathogenic Gram-negative bacteria (see Fig. 1.2). TTSSs are anchored to the bacterial inner and outer membranes via a basal body that is composed of "rings" made up of largely three conserved proteins [14]. From the apical side of the basal body, a rigid structure termed the "needle" protrudes outwards (purple in Fig. 1.2). It is composed of units of a single conserved protein that assemble into a helical structure and hence the interior of the needle forms a hollow channel [14]. Due to their appearance, TTSSs are sometimes also termed injectisomes. Proteins forming the tip of the injectisome are present at the distal end of the needle [15] (yellow in Fig. 1.2). Upon contact with a eukaryotic

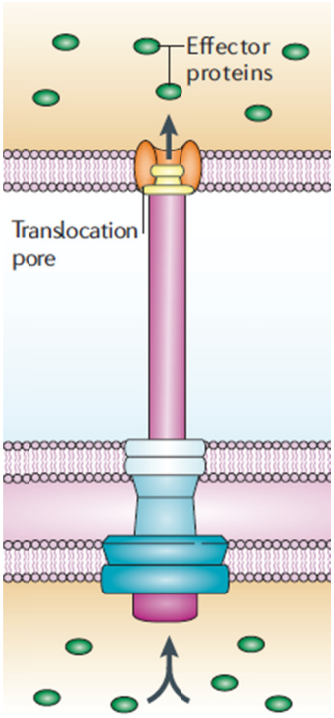

Fig. 1.2 | Illustration of an injectisome.
The apparatus is anchored to inner and outer membranes through ring-like subunits. The needle (purple) contains a hollow channel through which effector proteins (green) are secreted. [4]

host cell, translocator proteins (SipB and SipC in *S*. Typhimurium TTSS-1) are thought to be secreted through the channel within the needle of the apparatus and form a translocation pore ("translocon") within the host cell membrane (orange in Fig. 1.2). The tip proteins thereby act as molecular adaptors between translocon and injectisome [14]. The resulting direct connection from the bacterial interior to the host cell's cytoplasm is abused by the bacteria to translocate several effector proteins (green in Fig. 1.2), which facilitate bacterial survival within their hosts in different ways. *Yersinia* species for example employ injectisomes to interfere with inflammatory signaling in cells of the immune system and to destroy hostile phagocytes [16].
In *Salmonella* species, injectisomes have different functions. Pathogenic *S*. Typhimurium strains possess two type III secretion systems that are encoded on two separate chromosomal *Salmonella* pathogenicity islands (SPI-1 and SPI-2). The type III secretion system 1 (TTSS-1) is critical for the entry into host cells (see section 1.4). It is expressed in a bistable mode within a population of infectious bacteria [17] and mediates invasion of individual bacteria into non-phagocytic epithelial cells [18]. The type III secretion system 2 (TTSS-2) is involved in establishing a cellular compartment termed the "*Salmonella*-containing vacuole" (SCV) that protects the bacteria from lysosomal degradation and hence is indispensable for intracellular survival and systemic infections [18].

1.3. Small GTPases and their functions in actin dynamics

The Ras superfamily of small GTPases contains five protein subfamilies (Rab, Rho, Ras, Ran and Arf) that are composed of enzymes that are similar to the α subunit of G proteins [19]. In general small GTPases are thought to function as "molecular switches" [20]: when associated with GTP, they are present in an "on" state while the hydrolysis of GTP to GDP converts them into an "off" state [20]. Small GTPases have an intrinsic GTP hydrolysis activity, which is however relatively weak [19]. Their activity is largely regulated by a variety of cellular enzymes. Guanine nucleotide exchange factors (GEFs) catalyze the substitution of GDP with GTP and thereby promote activation of small GTPases [21]. GTPase activating proteins (GAPs) on the other hand enhance the intrinsic GTP hydrolysis and lead to the inactivation of GTPases [22]. Many members of the Ras superfamily are associated with membranes. The majority of small GTPases belonging to the Rac and Rho subfamilies are posttranslationally coupled to an isoprenoid moiety by the enzymatic activity of either geranylgeranyltransferase I (GGTase-I) or farnesyltransferase (FTase) [19]. Proteins of the Rab subfamily on the other hand are commonly modified by geranylgeranyltransferase II (GGTase-II), which has also been termed Rab

geranylgeranyl transferase [19]. The geranylgeranyl or farnesyl moieties serve as "lipid anchors" that are inserted into membranes and thereby retain small GTPases at cellular membranes.

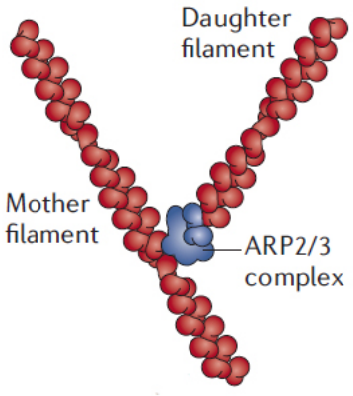

Fig. 1.3 | The Arp2/3 complex nucleates actin polymerization. The complex is composed of seven protein subunits. Upon activation, it catalyzes the polymerization of new actin side branches within existing filaments. [5]

Small GTPases are involved in the regulation of very diverse cellular processes including vesicle trafficking, cell cycle progression and the organization of the cytoskeleton [19]. Some Rho GTPases are important regulators of actin dynamics. Cdc42 has been found to promote formation of filopodia in cultured cells [23]. It targets downstream proteins including Wiskott-Aldrich syndrome protein (WASP) and mDia2 [24]. WASP in turn is an activator of the actin-related protein-2/3 (Arp2/3) complex (see Fig. 1.3). This complex is composed of seven protein subunits, including two that are closely related to G-actin [5]. The Arp2/3 complex is thought to nucleate the polymerization of new actin filaments from pre-formed ones and thus is an important organizer of actin elongation and branching [5]. The signaling pathway of Rac1, another Rho GTPase, converges with that from Cdc42 at the level of the Arp2/3 complex. The small GTPase Rac1 plays a prominent role in the formation of lamellipodia and is involved in phagocytosis through the induction of plasma membrane extensions [25]. Rac1 targets, amongst others, the WASP-family verprolin-homologous (WAVE) protein [24]. As the name suggests, analogously to WASP, WAVE acts as an activator of the Arp2/3 complex and thereby stimulates actin nucleation.

1.4. Effector proteins secreted with TTSS-1

Some *S.* Typhimurium effector proteins that are secreted with TTSS-1 are termed the key players of the invasion process as they are most potent to mediate invasion into epithelial cells (see Fig. 1.4). SipA and SipC both contain domains that directly interact with actin. SipC, which is also a component of the TTSS-1 translocon, contains two catalytic domains. The C-terminal domain promotes the polymerization of F-actin while the N-terminal domain catalyzes the cross-linking of filaments [26]. SipA supports the activity of SipC by directly stabilizing F-actin and thereby decreasing the concentration of G-actin that is needed for elongation [27, 28]. SopE and SopE2 both act as Guanine nucleotide exchange factors (GEFs) for Rho GTPases. With their GEF activities, SopE and SopE2 convert the GDP-bound, inactive forms of these GTPases to the active, GTP-bound forms: SopE activates both Cdc42 and Rac1 [29] whereas the activity of SopE2 seems to be restricted to Cdc42 [30]. These events lead to downstream signaling and activation of the Arp2/3 complex. This protein complex in turn binds to pre-formed actin filaments and enhances their elongation and branching [31], thus leading to plasma membrane protrusions ("ruffling") (see section 1.3). The effector protein SopB indirectly also supports membrane ruffling. It functions as a phosphatidylinositol phosphatase [32] and cleaves phosphatidylinositols to yield cellular secondary messengers that promote Arp2/3 recruitment [30]. SptP acts as GAP for Cdc42 and Rac1 and reverses the membrane ruffles introduced by other effector proteins [33] (see section 1.5).

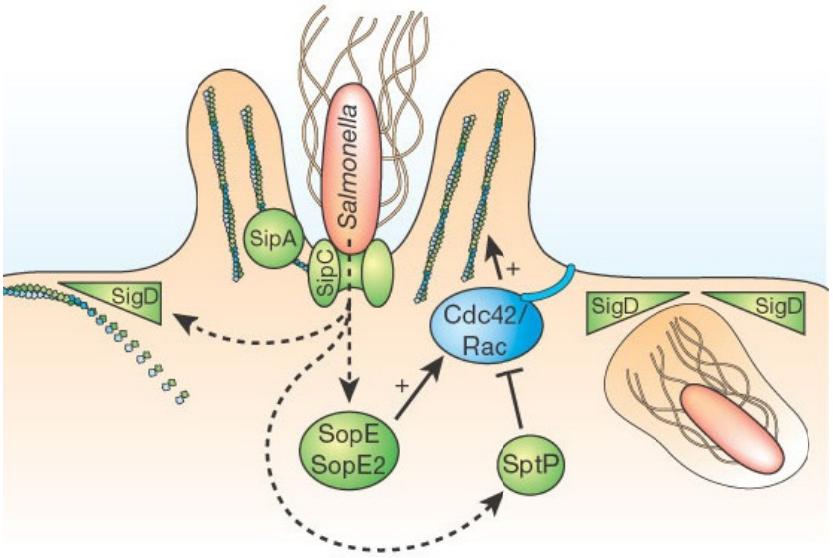

Fig. 1.4 | Overview of effector proteins that are secreted with TTSS-1. SipA and SipC bind actin directly and promote polymerization of F-actin. SopE and SopE2 both act as GEFs for Rho GTPases. SopE activates Cdc42 and Rac1 while SopE2 function is restricted to Cdc42. SptP is a GAP and antagonizes the effects induced by SopE and SopE2. SopB (denominated SigD in the figure) cleaves phosphatidylinositols and the resulting substrates support actin filament elongation. The changes in actin dynamics ultimately lead to host cell invasion of *S.* Typhimurium. [7]

1.5. A closer look at *Salmonella* outer protein E (SopE)

The effector protein SopE consists of 240 amino acids. It contains a C-terminal catalytic GEF domain and N-terminal sequences that are essential for translocation of the protein (see Fig. 1.5). The first 15-20 N-terminal amino acids are indispensable for proper secretion [34, 35]. Furthermore, the chaperone InvB is also necessary for translocation of SopE to host cells and binds to a region between amino acids 30-54 from the N-terminus [34]. Screenings of *S.* Typhimurium isolates have shown that SopE is encoded by a rather small minority of natural strains while many epidemic strains encode it [36]. SopE is obviously one of the most potent invasion-promoting effectors. Mutants encoding SopE but lacking SipA, SopB and SopE2 invade almost as efficiently as wildtype strains [1]. The effector SptP is a counter player of SopE, acting as GTPase activating factor (GAP) of Rac1 and Cdc42 [33]. Temporal regulation of the respective effector activities is thereby crucial. SopE is degraded in a proteasome-dependent manner shortly after translocation while SptP persists for a longer time period [37]. Thus, SptP leads to inactivation of Rac1 and Cdc42 after bacterial entry into the host cell and thereby to a recovery of the cytoskeletal organization. Furthermore, while cellular concentrations of SopE decrease quickly after infection through proteasomal degradation, SopE has been found to associate with SCVs *in vitro* [38] and to accumulate around individual bacteria in infected cultured cells up to 8 h post-infection [39]. Interestingly, a truncated version of the effector protein containing only the first 100 amino acids and therefore lacking the catalytic GEF domain ($SopE_{1-100}$) still accumulates around intracellular bacteria, while a version with the first 60 amino acids ($SopE_{1-60}$) does not anymore [39].

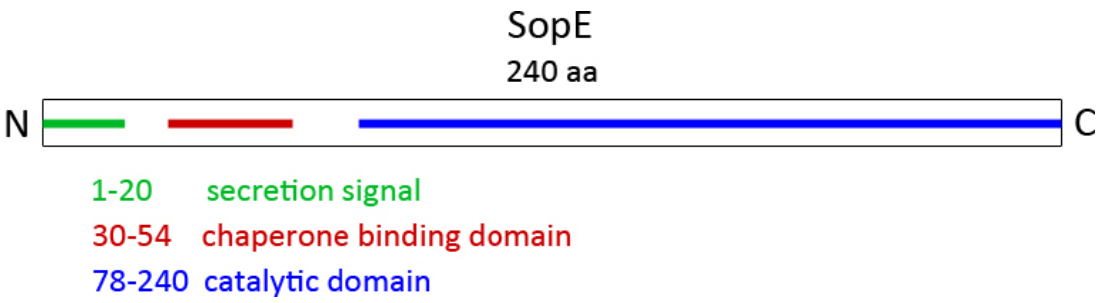

Fig. 1.5 Different domains of SopE. The protein consists of 240 amino acids. The N-terminus contains sequences that are critical for secretion (green) and chaperone binding (red). The C-terminal part of the protein contains the catalytic GEF domain (blue).

1.6. Different steps during *Salmonella* infections

The time course of *S.* Typhimurium infections can be divided into different steps [1]. Bacteria first need to get in close proximity to eukaryotic cells in order to insert their TTSS-1 into the host cell membrane and thereby irrevocably "dock" to the cell surface. This stable association allows injection of effector proteins directly into the host cell's cytoplasm. These effectors manipulate the cell's actin signaling network either directly or indirectly [30] (see section 1.4) and lead to plasma membrane ruffling that surround the bacteria. Upon membrane closure the bacteria become completely enclosed and are present intracellularly within vesicles that have been termed "*Salmonella*-containing vacuoles" (SCVs). At early stages of infections SCVs are associated with markers of early endosomes such as Rab5c and EEA1 [40]. The SCVs migrate from the peripheral regions of the cells towards the nuclei within 1-4 h [41] and gradually acquire late endosomal and lysosomal markers such as Rab7 and Lamp1 [42]. Simultaneously the lumen of the vesicle continuously acidifies to a pH between 4 and 5 [43].

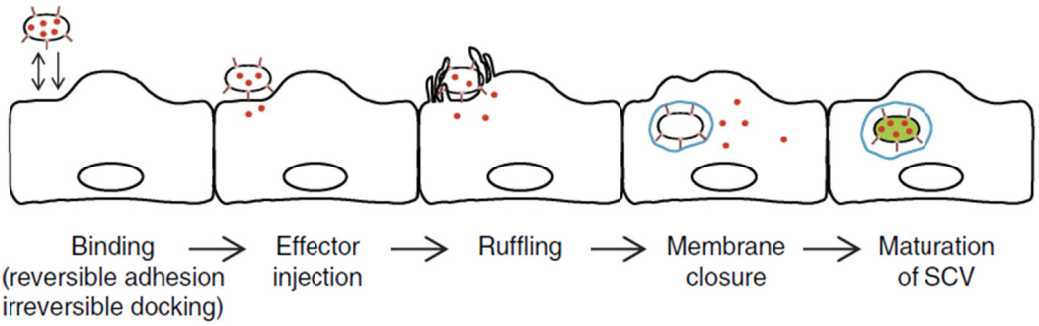

Fig. 1.6 | Sequence of events during *Salmonella* infections. Bacteria assemble translocons in host plasma membranes in order to irreversibly dock and inject effector proteins. Bacterial effectors induce actin polymerization and cell ruffling, leading to uptake of the bacteria. Within SCVs, *Salmonella* actively participates in the modeling of the vesicle to escape lysosomal degradation. [1]

S. Typhimurium actively controls the maturation of the SCV. This leads, for example, to the absence of some endolysosomal markers such as the mannose-6-phosphate receptor on the surface of the SCV [44]. The pathogen achieves this in part through the induction of TTSS-2 expression and secretion of SPI-2 effectors. SifA, one of the best-characterized SPI-2 effectors, is involved in the generation of filamentous membrane extensions of the SCV [45]. These "*Salmonella*-induced filaments" (Sifs) are anchored to microtubuli and are present in cultured cells 4-6 h post-infection [40]. Simultaneously with Sif formation bacterial replication is initiated.

1.7. Importance of TTSS-1 effectors after invasion

TTSS-1 effector proteins, which were thought to be important exclusively in the early phases of infection, have recently been shown to participate in later phases of infection as well. During the first few hours post-infection, SopB [46], SipA [47], SopE and SopE2 [39] have been found to be accumulated around intracellular bacteria. Furthermore SipC, which is a component of the TTSS-1 translocon, has been shown to directly participate in the recruitment of Lamp1 to the SCVs [48]. *S*. Typhimurium mutants not expressing TTSS-1 are severely impaired in the control of SCV maturation and intracellular replication [49], indicating that the effectors that are important for invasion are additionally involved in the control of later stages of infection.
However, the precise functions of these effectors on the SCVs remain unknown. Furthermore, for most of these proteins it has not been investigated how the differential localization is regulated and how they are recruited to SCVs. Research on the inositol phosphatase SopB has advanced to provide some answers to those questions. At early time points of infection the protein localizes predominantly to the plasma membrane of the host cell, where it cleaves phosphoinositides and activates signaling pathways that lead to acting remodeling [32]. Inside the host cell SopB gets ubiquitinated by cellular enzymes. This modification gradually leads to a redistribution of the protein towards SCVs [46, 50]. *S*. Typhimurium encoding versions of SopB that lack the sequences necessary for ubiquitination do not have accumulated SopB around SCVs and are dramatically reduced in their capacity for intracellular replication [51]. Similarly, bacteria lacking SipA [47], SopE and SopE2 (P. Vonaesch, personal communication) also seem to have deficiencies in their ability for replication.

1.8. Question of interest

For most *Salmonella* TTSS-1 effector proteins it has not yet been elucidated how they bind to SCVs. One of these effectors is the Guanine nucleotide exchange factor SopE. There are different possibilities how SopE could bind to SCVs. In this study we addressed the question if the interaction (i) originates from a posttranslational modification of the effector protein within host cells or (ii) results from a direct interaction of SopE with lipids of the SCV. Furthermore, we investigated if SopE is continuously synthesized once *S*. Typhimurium has successfully invaded its host cell.

2. Materials and Methods

2.1. Strains and plasmids

Table 2.1 | Overview of strains and plasmids

	Notation	Genotype	Comments	Reference
Bacterial strains	SB300	*Salmonella enterica* subspecies I serovar Typhimurium SL1344	May contain point mutations (strain was isolated after mouse passage).	[52]
	M708	SB300 Δ*sopB,* Δ*sopE,* Δ*sopE2,* Δ*sipA, sseD::aphT*	Deletion of the four key SPI-1 effectors, no functional TTSS-2.	S. Hapfelmeier
	SB245	SB300 *(sipA-sptP)::aphT, fliGHI::Tn10*	Strain for increased secretion of effectors.	K. Kaniga
	SB875	SB300 *sopE::sopE-M45*	Chromosomal *sopE* tagged with adenoviral M45 epitope [29, 53].	W.-D. Hardt
	DH5α	*Escherichia coli* DH5α; see ref. for more details	*E. coli* strain commonly used for highly efficient transformation.	[54]
Plasmids	pM965	*rpsM*^{p}-GFP*mut2* in pWKS30 backbone	Constitutive GFP expression.	[55]
	pM438	$SopE_{1-240}$-M45 in pACYC184 backbone	Complete *sopE* ORF fused to the M45 epitope, expressed from native *sopE* promoter.	[56]
	$pMSopE_{100}$	$SopE_{1-100}$-M45 in pACYC184 backbone	Truncated version of pM438: deletion of SopE residues 101-240.	P. Vonaesch
	$pMSopE_{100}$-His_6	$SopE_{1-100}$-M45-Leu-His_6 in pACYC184 backbone	$pMSopE_{100}$ with insertion of $(His)_6$ between M45 epitope and stop codon.	This report
	$pM438_{S-A}$	SopE *Ser_{72}::Ala-M45*		This report
	$pM438_{T1-A}$	SopE *Thr_{64}::Ala-M45*		This report
	$pM438_{T2-A}$	SopE *Thr_{79}::Ala-M45*		This report
	$pM438_{K1-A}$	SopE *Lys_{81}::Ala-M45*		This report
	$pM438_{K2-A}$	SopE *Lys_{84}::Ala-M45*		This report
	$pM438_{K1,2-A}$	SopE (*Lys_{81}::Ala Lys_{84}::Ala*)*-M45*		This report
	pSB1180	SopE-Kinase site in pBAD backbone	*sopE* fused to a Protein kinase A target site (RRASV) [29, 57]. Arabinose inducible.	S. Mirold
	pSB1181	SopE-Kinase site-M45 in pBAD backbone	*sopE* fused to a Protein kinase A target site (RRASV) and an M45 epitope. Arabinose inducible.	[29]
	pGEX-2TK	*tac*^{p}-GST(p)	IPTG-inducible vector with phosphorylation site, commonly used for GST-fusion proteins.	GE Life Sciences
	pM2120	*rpsM*^{p}*-mCherry* in pBR322 / pBAD backbone	Constitutive mCherry expression.	P. Songhet
	pM1492	*rpsM*^{p}*-RedStar* in pWKS30 backbone	Constitutive RedStar RFP expression.	L. Häberli
	pCJLA-RFP	*lac*^{p}*-RFP* in pACYC184 backbone	Constitutive RFP expression.	C. Jakobi
	pCLR7	*C 10E*^{p}*-dsRedC*. In pBAD backbone	Constitutive DsRed expression	D. Bumann

2.2. Bacterial culture

Bacteria were streaked out from glycerol stocks onto agar plates containing lysogeny broth (LB) supplemented with the appropriate antibiotics (a list of all solutions and chemicals can be found below) and were incubated at 37°C over night. Single colonies were inoculated into 3 ml fresh LB 0.3 M NaCl containing the appropriate antibiotics and incubated for 12 h at 37°C on a rotating wheel. Cultures were then diluted 1/20 in 3 ml fresh LB 0.3 M NaCl without any antibiotics and incubated during 4 h at 37°C on a rotating wheel.

2.3. Cell culture

HeLa-Kyoto cells were cultured in DMEM with 10% FCS and 50 mg/l streptomycin in a HERAcell® 240 cell incubator (Thermo Scientific) at 37°C, 5% CO_2 to 70-80% confluency. The media for HeLa cells expressing either Rac1-GFP or Lifeact-GFP were supplemented with 500 µg/ml G-418 sulphate; the medium for Lifeact-GFP cells contained additionally 10 mM non-essential amino acids. After the cells had reached a passage of 15, new cells from the liquid nitrogen stock were thawed. Inhibitors and antibiotics were added as indicated in the respective experiments. Cells were observed with an Axiovert 40 CFL inverted microscope (Zeiss) and counted with a Neubauer improved hemocytometer (Hecht Assistent).
Murine hybrid cells of monoclonal specificity for the M45 epitope (referred to as M45 hybridomas in this report) were thawed from a liquid nitrogen stock and cultured in RPMI-1640 that was supplemented with 15% FCS (with low IgG levels), 2 mM L-Glutamine, 100 U/ml penicillin and 0.1 mg/ml streptomycin. Cells were diluted to $2.5x10^7$ in 15 ml fresh medium and pipetted into the cell compartment of a CELLine CL 1000 bioreactor (Integra). 1000 ml nutrient medium (same as above but without FCS) was added to the nutrient compartment and the bioreactor was incubated at 37°C, 5% CO_2. Every three to five days the cell supernatant containing immunoglobulins was harvested, cells were diluted ten-fold and the nutrient medium was replaced. After multiple passages the recovered supernatants were pooled and aliquots were freezed at -20°C.

2.4. Cell infection and fluorescent staining

Unless otherwise indicated, 40.000 cells in 0.5 ml medium were added to glass coverslips in 24 well plates 20–24 h prior to infection. Bacterial 4 h cultures were diluted 1/16 in fresh LB 0.3 M

NaCl and 100 µl of the dilution were added to each well of the 24 well plates. The plates were placed into the incubator (37°C, 5% CO_2) for 10 min, washed with pre-warmed fresh medium and incubated for additional 50 min. Cells were fixed in pre-warmed fixing solution during 15 min, washed three times with 4% sucrose solution, incubated in 20% sucrose solution for 10 min, permeabilized in 0.1% Triton X-100 for 5 min and incubated in blocking buffer for 1 h. Dilutions of antibodies and fluorescent chemicals (DAPI and Alexa-647-phalloidin) were prepared in blocking buffer and added in 50 µl droplets to plastic paraffin films. Coverslips were incubated on these droplets for 1 h (primary antibodies) or 45 min (secondary antibodies and fluorescent chemicals) respectively, re-transferred to the wells and washed four times with PBS. Coverslips were mounted to microscope slides with 5 µl Mowiol.

2.5. Microscopy, quantification and analysis

Image stacks were acquired with an Axiovert 200 m inverted microscope (Zeiss) that was equipped with an Ultraview confocal head (Perkin Elmer) and a krypton-argon laser (643-RYB-A01, Melles Griot) using a 100x oil immersion objective (PLAN-Apochromat, Zeiss) with a numeral aperture of 1.4 and Z intervals of 0.2 µm.

Images were analyzed with Volocity 3D Image Analysis Software (Version 6, Perkin Elmer). For quantification of fluorescence within whole cells, the mean fluorescence intensity of the cell area was measured over the entire stack. Average background fluorescence intensity was then measured over a similar area in a cell-free region of the field of view and subtracted. The resulting value was divided by the number of bacteria that had infected the cell in order to get a normalized value. For quantification of fluorescence around individual *Salmonellae*, an area surrounding the bacteria was selected and the mean fluorescence intensity was corrected for background fluorescence by subtracting the average fluorescence intensity of a region next to the bacterium within the same host cell.

The measured values were plotted to graphs with the software Prism (Version 5, GraphPad) and two-tailed, unpaired t tests were used for analysis of the values.

2.6. Time-lapse microscopy

200.000 cells in 2 ml medium were seeded into glass-bottom dishes (MatTek) 20 h prior to microscopy. Shortly before imaging, the medium was exchanged for pre-warmed HBSS with 10% FCS, 10 mM HEPES and dishes were mounted to a pre-warmed (35°C) specimen holder.

Infection was carried out with 100 µl of 16-fold diluted bacterial 4 h-cultures. After acquisition of each image, a delay of 8-10 s was integrated to minimize cellular stress due to light exposure, as had been done before [58].

2.7. Plasmid transformation

Aliquots of electrocompetent cells were prepared as follows: 2 ml stationary phase cultures were diluted in 100 ml fresh LB medium in 1 L Erlenmeyer flasks and incubated in a shaking (250 rpm) incubator at 37°C until cells had reached an optical density (OD_{600}) of 0.5-0.8. Cultures were then incubated on ice for 30-60 min and centrifuged at 4000 rpm, 4°C for 20 min. Cells were washed three times with 25 ml cold ddH_2O and taken up in 5 ml cold 10% glycerol in ddH_2O. After centrifugation at 4000 rpm, 4°C for 15 min the pellets were re-suspended in 500 µl of cold 10% glycerol solution. Aliquots of 90 µl were prepared and flash-frozen in liquid nitrogen.
Electroporation was carried out by mixing 2-5 µl of purified plasmid DNA (50-200 ng) with an aliquot of electrocompetent cells in 1 mm electroporation cuvettes (BTX). Pulsing at 18 kV/cm was performed with a Gene Pulser Xcell™ (Bio-Rad). Immediately after electroporation cells were transferred to 800 µl fresh LB and incubated for 45-60 min at 37°C, 1000 rpm in a shaking incubator. Bacteria were then spread onto LB agar plates containing the appropriate antibiotics and incubated at 37°C over night.

2.8. Polymerase chain reactions (PCR) and molecular cloning

All plasmids used for polymerase chain reactions were transformed into and harvested from *E. coli* DH5α with NucleoSpin® Plasmid preparation kits (Macherey-Nagel). Experimental procedures for site-directed mutagenesis of single amino acids (alanine substitutions) and overlap extension PCR cloning are based on previous protocols [59, 60]. For each reaction, roughly 50 ng DNA were mixed with 10 µM forward and reverse primers, 4 mM deoxynucleoside triphosphates and 2.5 units Pfu Polymerase in Pfu Buffer. Programs used with the thermal cycler are listed in Table 2.3.
Primers were designed with the software Clone Manager (Version 9, Professional Edition, Sci-Ed softwares) and ordered from the company Microsynth in desalted form without any modifications (see Table 2.2 for sequences). All constructed plasmids were sequenced in order to verify the successful introduction of the mutations. For sequencing reactions 8 µl purified

plasmid DNA (≈250 ng) were mixed with 2 µl primer solution (20 pmol) and sent to Microsynth for sequencing.

Table 2.2 | Primers used for plasmid construction

Constructed plasmid	Forward primer sequence	Reverse primer sequence
pM438$_{S\text{-}A}$	5'-CGA GGA AGC GCA GCT GAG GGC CGG G-3'	5'-CCC GGC CCT CAG CTG CGC TTC CTC G-3'
pM438$_{T1\text{-}A}$	5'-CAC TGA GTC TTC TGC AGC ACA CTT TCA CCG AG-3'	5'-CTC GGT GAA AGT GTG CTG CAG AAG ACT CAG TG-3'
pM438$_{T2\text{-}A}$	5'-GAG GGC CGG GCA GTG TTG GCA AAT AAA GTC GTT AAA G-3'	5'-CTT TAA CGA CTT TAT TTG CCA ACA CTG CCC GGC CCT C-3'
pM438$_{K1\text{-}A}$	5'-GGC CGG GCA GTG TTG ACA AAT GCA GTC GTT AAA GAT TTT ATG C-3'	5'-GCA TAA AAT CTT TAA CGA CTG CAT TTG TCA ACA CTG CCC GGC C-3'
pM438$_{K2\text{-}A}$	5'-CAG TGT TGA CAA ATA AAG TCG TTG CAG ATT TTA TGC TTC AAA CGC TC-3'	5'-GAG CGT TTG AAG CAT AAA ATC TGC AAC GAC TTT ATT TGT CAA CAC TG-3'
pM438$_{K1,2\text{-}A}$	5'-CAG TGT TGA CAA ATG CAG TCG TTG CAG ATT TTA TGC TTC AAA CGC TC-3'	5'-GAG CGT TTG AAG CAT AAA ATC TGC AAC GAC TGC ATT TGT CAA CAC TG-3'
pMSopE$_{100}$-His$_6$	5'-CGG ATC CTC CAC CAT CAC CAT CAC CAT CTG TAG AGT CGA CCG ATG CCC TTG AG-3'	5'-TCG ACT CTA CAG ATG GTG ATG GTG ATG GTG GAG GAT CCG CGT CTC TGT CTC-3'

Table 2.3 | PCR programs used with thermocyclers

Site-directed mutagenesis (single amino acids)		Overlap extension PCR cloning (His$_6$ insertion)	
Temperature	**Duration**	**Temperature**	**Duration**
95°C	30 s	95°C	3 min
95°C	30 s |	95°C	50 s |
55°C	1 min | 16 cycles	55°C	1 min | 18 cycles
68°C	5 min |	68°C	5 min 30 s |
68°C	7 m in	68°C	7 min

2.9. RNA interference

RNA interference was performed in 24 well plates. Glass coverslips were placed into the wells and 10 µl of the corresponding siRNA (1 µM) were pipetted next to the coverslips. For control, siRNA targeting Polo-like kinase (PLK) was added to two wells. Lipofectamine was diluted 200-fold in OptiMem and incubated for 20 min at room temperature. 40 µl of the dilution were then added to each well, mixed with the siRNA and incubated for another 20 min at room temperature. Then, 8000 cells in 0.5 ml were added to each well. After three days in the

incubator, successful interference was analyzed by monitoring cell death in the wells that contained cells with siRNA targeted against PLK. Cells were infected, fixed and stained according to section 2.4.

2.10. Purification of SopE from bacterial culture supernatant

Single colonies of strain SB245 harboring plasmid pSB1180, pSB1181 or pM438 respectively were each inoculated in quadruplicates into four tubes containing 3 ml LB with the corresponding antibiotics and incubated for 12 h at 37°C with constant rotation. 20-fold diluted subcultures were prepared with 3 ml fresh LB and incubated for 3 h at 37°C. Then, L-arabinose to a concentration of 0.2% and β-mercapto ethanol to a concentration of 3 mM were added and the cultures were incubated for another 1.5 h at 37°C. Cultures of the same strain were pooled (12 ml in total per strain) and centrifuged 30 min at 15.000 rpm, 4°C in a Sorvall RC-5B high speed centrifuge (rotor SS-34, precooled to 4°C). Supernatants were passed through 0.22 µm sterilization filters and proteins were concentrated with Amicon® Ultra-4 10K (nominal molecular weight limit: 10 kDa) centrifugal filter units (Millipore) by centrifugation for 15 min at 4000 rpm, 4°C. After a final wash run with PBS, aliquots (20 µl each) of the concentrated proteins were snap-frozen in liquid nitrogen and stored at -80°C.

2.11. Purification of glutathione S-transferase (GST)

Single colonies of *E. coli* DH5α harboring plasmid pGEX-2TK were inoculated into four tubes each containing 5 ml LB with ampicillin and incubated for 12 h at 37°C on a rotating wheel. The cultures were then pooled and added to 180 ml fresh LB supplemented with ampicillin and incubated at 37°C. After the culture had reached an OD_{600} of 0.7, IPTG to a final concentration of 1 mM was added in order to induce the expression of GST. After culturing the cells for another 3.5 h at 37°C, they were collected by centrifugation for 20 min at 4000 rpm, 4°C. Pellets were re-suspended in 20 ml cold binding buffer and lysed in two passages through a French pressure cell press (1000 PSI). The lysate was centrifuged 30 min at 15.000 rpm, 4°C in a Sorvall RC-5B high speed centrifuge (rotor SS-34, precooled to 4°C) to remove cell debris and non-lysed cells. The supernatant was added to an equilibrated Glutathione Sepharose 4B column and washed twice with GST binding buffer before proteins were released in GST elution buffer. The eluted fractions were concentrated with Amicon® Ultra-4 10K centrifugal filter units (15 min at

4000 rpm, 4°C) and washed with PBS. Aliquots (20 µl) were shock-frozen in liquid nitrogen and stored at -80°C.

2.12. SDS-Polyacrylamide gel electrophoresis and Western blot analysis

Resolving gels were prepared with an acrylamide concentration of 12% in 0.5 M Tris-HCl, pH 8.8. Stacking gels were prepared with 3.5% acrylamide in 0.5 M Tris-HCl, pH 6.8. For both gels, 0.1% SDS, 0.1% ammonium persulfate and 0.01% TEMED were added to the solutions. Protein samples were diluted in Lämmli sample buffer and heated to 94°C for 5-10 min. 15 µl of the denatured samples were added to the gel wells. As protein marker, 5 µl of Benchmark™ pre-stained protein ladder (Invitrogen) were included. Proteins were separated in SDS-PAGE running buffer at a voltage of 120 V (electrode distance: ≈15 cm).
For Western blot analysis, proteins were transferred to cationized nylon membranes (Bio-Rad) (1 h, 15 V). Membranes were blocked with 5% milk powder in PBS-T (0.1 % Tween-20) for 1 h at room temperature or over night at 4°C. Primary and secondary (HRP-tagged) antibodies were added in blocking solution for 1 h at room temperature, followed by three washes in PBS-T without milk powder for 5 min each. Chemiluminescence reactions were initiated by addition of detection reagents for 2 min to the membranes. For visualization, x-ray films (Fujifilm) were exposed and then developed in an automated x-ray film developer (Fujifilm).

2.13. Protein-lipid binding assays on PIP membranes

Kinase reactions were adapted from previous protocols [29, 57]. For analytical reactions, approximately 0.5 µg protein were mixed with 2 units Protein Kinase A (catalytic subunit) in Kinase buffer supplemented with 1 mM DTT (freshly prepared in order to prevent oxidation). 50 µCi γ-^{32}P-ATP were added (total volume: 80 µl) and the reaction was incubated at 37°C for 15 min. Then, 27 µl 4x Lämmli sample buffer were added to each reaction and the solution was heated to 94°C for 5 min. Proteins were separated on SDS-polyacrylamide (12%) gels until the tracking dye had reached two thirds of the gel path in order to prevent radioactive ATP from flowing into solution. Gels were transferred to filter papers and incorporation of ATP was measured with a PhosphorImager® scanning instrument (Molecular Dynamics).
For lipid binding assays, PIP Strip™ membranes (Echelon) were blocked with 3% BSA in PBS-T (0.1% Tween-20) for 16-18 h at 4°C. 2 µg protein and 10 units kinase catalytic subunit were mixed in Kinase buffer and 1 mM DTT. 80 µCi γ-^{32}P-ATP were added (60 µl total volume) and

reactions were incubated at 37°C for 15 min. The reactions were stopped by addition of 1 ml Kinase stop buffer and incubated on ice for 5 min. Protein reactions were diluted in 4 ml blocking solution and added to the membranes at room temperature for 1 h. Membranes were then washed four times with PBS-T and transferred to film cassettes (wrapped in plastic foil to prevent contamination). X-ray films (Fujifilm) were exposed and developed as described for Western blot analysis.

2.14. Subcellular fractionation

The experimental procedure was adapted from a previous study [46]. Kyoto cells were cultured in four 75 cm^2 cell flasks to roughly 80% confluency. Cells were infected with 1 ml undiluted 4h subcultures of M708 harboring plasmid pM438. After 10 min the cells were washed with pre-warmed DMEM/10% FCS and incubated for another 20 min at 37°C, 5% CO_2. Then, cells were washed twice with cold PBS and once with cold homogenization buffer. Cells were scraped off in 1.5 ml cold homogenization buffer and passed through a cell homogenizer containing an 8 µm bead in order to disrupt plasma membranes.

For microscopic analysis of SopE localization, 200 µl of the homogenate were centrifuged onto coverslips that had been covered with polylysine (5 min at 2000 rpm and 4°C). The homogenate was then fixed with 4% PFA and stained according to section 2.4.

For subcellular fractionation, homogenates were pooled and centrifuged for 15 min at 4000 rpm, 4°C in order to pellet a fraction containing undisrupted cells, bacteria, nuclei and cytoskeletal filaments of infected cells (designated fraction P). Pellets were resuspended in 400 µl Lämmli sample buffer and stored at 4°C. Supernatants were transferred to ultracentrifugation tubes and centrifuged for 45 min at 37.000 rpm, 4°C in a Beckman Coulter Optima LE-80K ultracentrifuge with rotor 70.1 TI (resulting in a centrifugal force of > 100.000 g). The supernatants, containing cytosolic proteins, fragments of plasma membranes and endoplasmic reticulum among others, were pooled and denominated fraction C. The pellets (containing organelles such as endosomes, lysosomes, mitochondria and peroxisomes; designated fraction M) were resuspended in 1 ml membrane buffer that was supplemented with either 0.15 M NaCl, 1 M NaCl, 0.1 M sodium carbonate (pH 11.5) without Tris or 1% Triton X-100. After 30 min incubation on ice the tubes were re-centrifuged as above. Supernatants were removed and saved for protein precipitation (see below). Pellets were washed once in membrane buffer and resuspended in 100 µl Lämmli sample buffer.

Proteins in fraction C and supernatants from fractions M were precipitated by addition of trichloroacetic acid to a concentration of 10% and incubation on ice for 30 min. Tubes were

then centrifuged for 15 min at 14.000 rpm, 4°C and pellets were resuspended in 100 µl Lämmli sample buffer each.
For Western blot analysis, fractions were run on a 12% SDS polyacrylamide gel and processed as described in section 2.12.

2.15. Chemicals and reagents

Table 2.4 | Overview of chemicals and reagents

Notation	Description	Supplier
Acrylamid	Acrylamid 4K, 40%	AppliChem
Alexa-647-Phalloidin		Molecular Probes
Ampicillin (Amp)	Final concentration: 100 µg/ml	AppliChem
APS	Ammonium persulfate	AppliChem
Chloramphenicol (Cm)	Final concentration: 30 µg/ml	AppliChem
DAPI	4',6-diamidino-2-phenylindole. Final concentration: 1 µg/ml.	Sigma-Aldrich
DMEM	Dulbecco's minimal essential cell medium (DMEM) with high glucose (4.5 g/l), phenol red and stable glutamine.	PAA Laboratories
DNA marker	GeneRuler™ DNA Ladder Mix. Range from 100 bp to 10 kbp.	Fermentas
Erythromycin (Em)	Final concentration: 25 µg/ml	AppliChem
Fetal calf serum (FCS)	FCS was heat-inactivated prior to use.	Gibco
G-418 sulphate	Final concentration: 500 µg/ml	PAA Laboratories
GGTI	GGTI-2147; a cell-permeable non-thiol peptidomimetic that acts as a potent and selective inhibitor of geranylgeranyltransferase I (GGTase I).	Calbiochem
Goat α-mouse Cy3	Cy3-conjugated goat α-mouse IgG. Dilution: 1/100.	Milan Analytica
Goat α-mouse HRP	HRP-conjugated goat α-mouse IgG. Dilution: 1/5000.	Sigma
Goat α-rabbit HRP	HRP-conjugated rabbit α-mouse IgG. Dilution: 1/5000.	Jackson
HBSS	Hank's buffered saline solution with $MgCl_2$ and $CaCl_2$.	Gibco
HEPES	Buffer solution, 1 M	PAA Laboratories
Kanamycin (Km)	Final concentration: 50 µg/ml	AppliChem
L-Glutamine	Final concentration: 2 mM	PAA Laboratories
Lipofectamine	Lipofectamine™ RNAiMAX Reagent.	Invitrogen
MG132	Proteasome inhibitor MG132	Calbiochem
Milk powder		Coop
Mowiol	Mowiol® 4-88	Sigma-Aldrich
NEAA	Non-essential amino acids: L-Ala, L-Asn, L-Asp, L-Glu, L-Gly, L-Pro and L-Ser	PAA Laboratories

OptiMem	OPTI-MEM® 1x	Invitrogen
PBS (for cell culture)	Dulbecco's phosphate buffered saline (1x) without calcium and magnesium.	PAA Laboratories
Protein Kinase A catalytic subunit	9 units/µg protein; isolated from bovine heart. Lyophilized powder was resuspended in 200 µl ddH_2O with 6 mg/ml DTT yielding a concentration of 0.1 µg protein / µl solution. Solution was freshly prepared prior to experiment.	Sigma-Aldrich
Protein marker	Benchmark™ pre-stained protein ladder. Range from 10-190 kDa.	Invitrogen
PYR-41	PYR-41; a cell permeable inhibitor of Ubiquitin activating enzyme (E1) with little or no activity against E2 and E3. Final concentration: 50 µM	Sigma-Aldrich
RPMI-1640	Roswell Park Memorial Institute (RPMI)-1640 cell medium without L-Glutamine, with Phenol Red.	PAA Laboratories
Streptomycin (Sm)	Final concentration: 50 µg/ml	AppliChem
TEMED	N,N,N',N'-Tetramethylethylenediamine	National Diagnostics
Tetracycline (Tet)	Final concentration: 12.5 µg/ml.	AppliChem
Triton-X100		Sigma-Aldrich
Trypsin-EDTA (TE)	0.05% Trypsin in 0.53 mM EDTA.	Invitrogen
Tween-20		National Diagnostics
Western Blot Detection Reagents	Amersham ECL™ Western Blotting Detection Reagents.	GE Healthcare

2.16. Solutions

Table 2.5 | Overview of prepared solutions

Notation	Description
Blocking solution	PBS supplemented with 3% BSA and 4% sucrose.
Carbonate membrane buffer	0.1 M sodium carbonate (pH 11.3) and 5 mM $MgCl_2$ in ddH_2O, filter-sterilized and supplemented with PhosSTOP phosphatase inhibitors (Roche) and complete protease inhibitors (Roche).
Coomassie stain	50% ethanol, 10% acetic acid, 2% Coomassie brilliant blue R250 in dH_2O.
Coomassie destain	30% acetic acid, 15% methanol in dH_2O.
Fixation solution	PBS supplemented with 4% PFA and 4% sucrose.
GST binding buffer	10% glycerol in PBS, autoclaved.
GST elution buffer	10% glycerol, 20 mM glutathione in PBS, filter-sterilized.
Homogenization buffer	50 mM imidazole (pH 7.4), 250 mM sucrose and 0.5 mM EDTA in ddH_2O, filter-sterilized and supplemented with PhosSTOP phosphatase inhibitors (Roche) and complete protease inhibitors (Roche).
Kinase Buffer	A 10x stock solution was prepared and autoclaved: 200 mM Tris-HCl (pH 7.4), 1 M NaCl, 120 mM $MgCl_2$ in ddH_2O.
Kinase Stop Buffer	1 mg/ml BSA, 10 mM Na_2HPO_4, 10 mM $Na_4P_2O_7$, 10 mM EDTA in ddH_2O.
Lämmli sample buffer	Fivefold concentrated stock solutions were prepared: 625 mM Tris, 6.25 M glycine,

	2.5% SDS in dH_2O.
LB 0.3 M NaCl	Lysogeny broth supplemented with NaCl: 0.3 M NaCl, 10 g/l tryptone and 5 g/l yeast extract in dH_2O. Aliquots were autoclaved.
Membrane buffer	20 mM Tris-HCl (pH 7.2) and 10 mM $MgCl_2$ in ddH_2O, filter-sterilized and supplemented with PhosSTOP phosphatase inhibitors (Roche) and complete protease inhibitors (Roche).
PBS	Tenfold concentrated stock solutions were prepared and autoclaved: 1.37 M NaCl, 27 mM KCl, 43 mM Na_2HPO_4, 18 mM KH_2PO_4 in dH_2O.
PBS-T	PBS supplemented with 0.1% Tween-20.
Pfu Buffer	Tenfold concentrated stock solutions were prepared: 200 mM Tris-HCl (pH 8.8), 100 mM $(NH_4)_2SO_4$, 100 mM KCl, 20 mM $MgSO_4$, 1% Triton X-100, 1 mg/ml BSA in ddH_2O.
SDS-PAGE running buffer	Tenfold concentrated stock solutions were prepared: 250 mM Tris, 2.5 M glycine, 1% SDS in dH_2O.
Sucrose solution (20%)	PBS supplemented with 20% sucrose.
Sucrose solution (4%)	PBS supplemented with 4% sucrose.
Trichloroacetic acid	250 g were added to 113 ml dH_2O.
Western Transfer Buffer	25 mM Tris-HCl (pH 8.3), 190 mM glycine, 20% methanol in dH_2O.

3. Results

3.1. Production of monoclonal α-M45-epitope antibodies

The *S*. Typhimurium strains that were used for infection in immunofluorescence experiments encoded SopE versions that were tagged with the M45 epitope of protein E4-6/7 from adenovirus [53]. This epitope had previously been found to be an efficient marker for immunostaining and Western blot analysis [29]. In order to produce fresh α-M45-epitope antibodies, murine hybridomas of M45 specificity were thawed and cultured in a bioreactor. Supernatants of the cell compartment were recovered and pooled. A part of the pooled supernatants was purified on a protein G column in order to investigate if this procedure improved the binding specificity of the antibodies. Both the unpurified as well as the purified supernatants were assayed for specificity to SopE-M45. To this end, overnight cultures of M708 harboring plasmid pM438 were lysed in Lämmli sample buffer and run on a gel, undiluted in one and tenfold diluted in a second lane. The gels were probed with different dilutions of unpurified or purified supernatant respectively in a Western blot assay (Fig. 3.1). As a negative control, a culture of *E. coli* DH5α harboring plasmid pGEX-2TK was also lysed in Lämmli sample buffer and included in a third gel lane. Furthermore, the flow-through of the Protein G column was also used for detection of SopE-M45 in order to determine whether the purification of the antibodies had been efficient.

Purified as well as non-purified antibodies bound exclusively to the M45-tagged SopE proteins (Fig. 3.1, A). No unspecific binding was observed (see lanes with DH5α lysates). Purified antibodies were able to detect the target epitope in higher dilutions: a 1/200 dilution still resulted in a thick band for undiluted *S*. Tm cultures, whereas a 1/100 dilution was enough to detect tenfold diluted cultures. Unpurified supernatant on the other hand detected tagged SopE from undiluted cultures when used in a 1/100 dilution. Tenfold diluted *S*. Tm cultures could still slightly be detected with a 1/10 dilution of the supernatant.

In order to confirm staining in cells and to determine the optimal dilution to be used for microscopy, HeLa cells were infected with M708 harboring plasmids pM438 (encoding SopE-M45) and pM965 (for constitutive GFP expression). After one hour the cells were fixed and stained with different dilutions of purified or non-purified α-M45 antibodies.

Immunoglobulins from unpurified supernatant bound intracellularly to epitopes around bacteria (Fig. 3.1, B). Staining with tenfold diluted supernatant resulted in an intense fluorescence signal. Dilutions up to 1/100 still led to specific staining. Higher dilutions than 1/75

however resulted in a loss of observable fluorescence intensity. 50-fold diluted supernatant resulted in an optimal signal-to-noise ratio, as determined by microscopic observation.
Purified antibodies were found to be localized around bacteria as well. A 1/500 dilution resulted in a distinctly lower signal intensity than a 1/200 dilution. 200-fold diluted purified antibodies are therefore recommended for use in experiments with immunofluorescence.

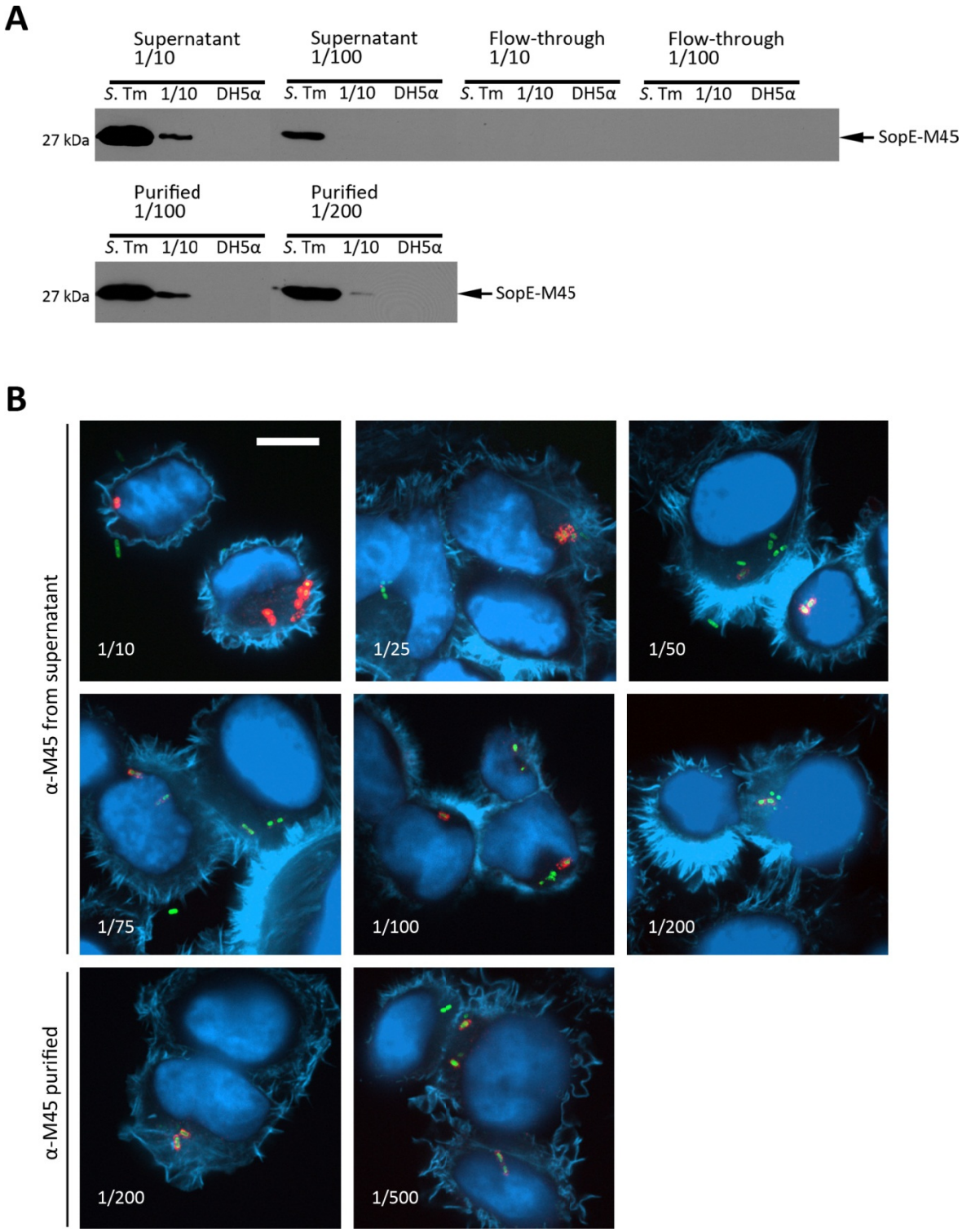

Fig. 3.1 | Determination of the optimal antibody dilutions for immunofluorescence analysis.
(A) Cultures of *S*. Typhimurium were run undiluted (*S*. Tm lane) or tenfold diluted (1/10 lane) on a gel. *E. coli* strain DH5α was included as a control. Western blot analysis was carried out with the indicated dilutions of M45 supernatant, purified antibodies or flow through of the protein G column.
(B) HeLa Kyoto cells were infected with an *S*. Tm strain encoding SopE-M45 and stained with different dilutions of the non-purified or purified antibodies. Green: *S*. Tm, red: SopE-M45, light blue: actin cytoskeleton, dark blue: nuclei. Scale bar: 10 µm.

3.2. Mutagenesis of conserved serine, threonine and lysine residues

In order to identify conserved amino acids, a sequence alignment of SopE and SopE2 was performed with the alignment tool LALIGN [61]. Within the region between amino acids 60 and 100, Thr_{64}, Ser_{72}, Thr_{79}, Lys_{81} and Lys_{84}, among other amino acids, were found to be conserved (Fig. 3.2). These residues may be hypothetical sites of posttranslational modifications such as phosphorylation or ubiquitination respectively.

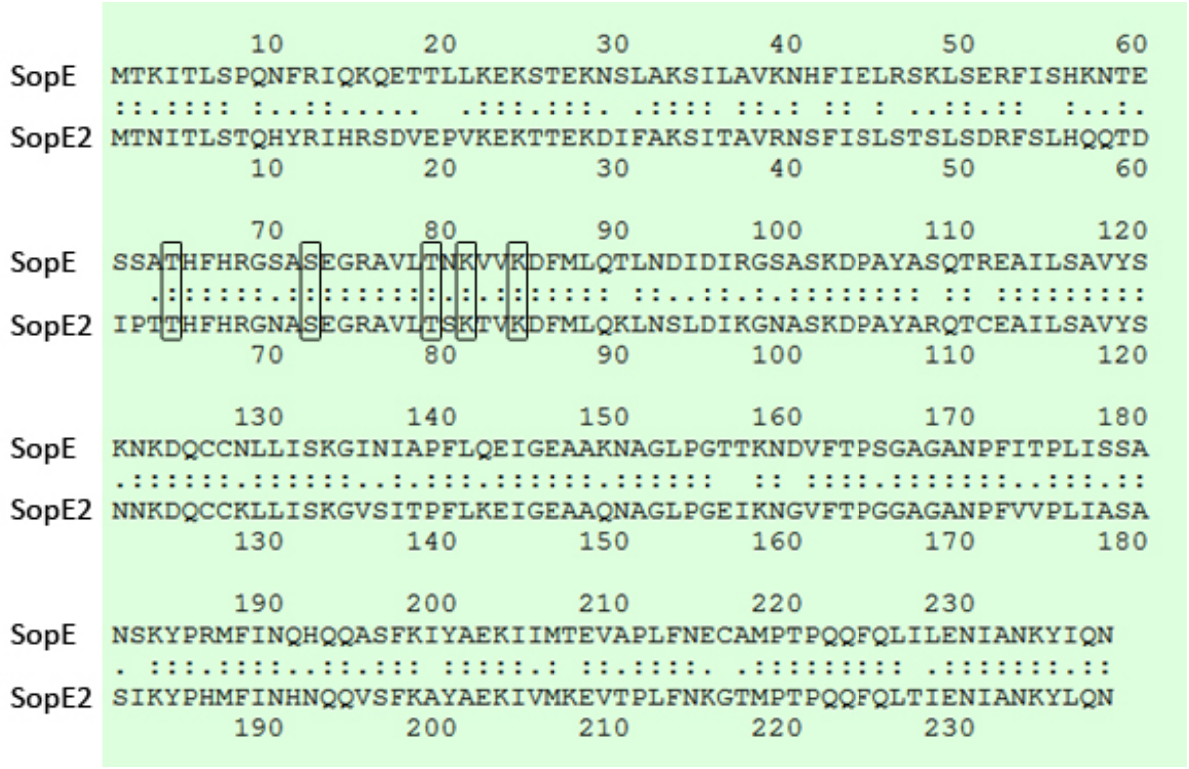

Fig. 3.2 | Alignment of SopE and SopE2 reveals conserved amino acids. Sequences of the proteins were obtained from the universal protein resource [3] and aligned with the LALIGN alignment tool. Three possible phosphorylation sites (T and S) and two possible acetylation sites (K) are conserved between residues 60 and 100.

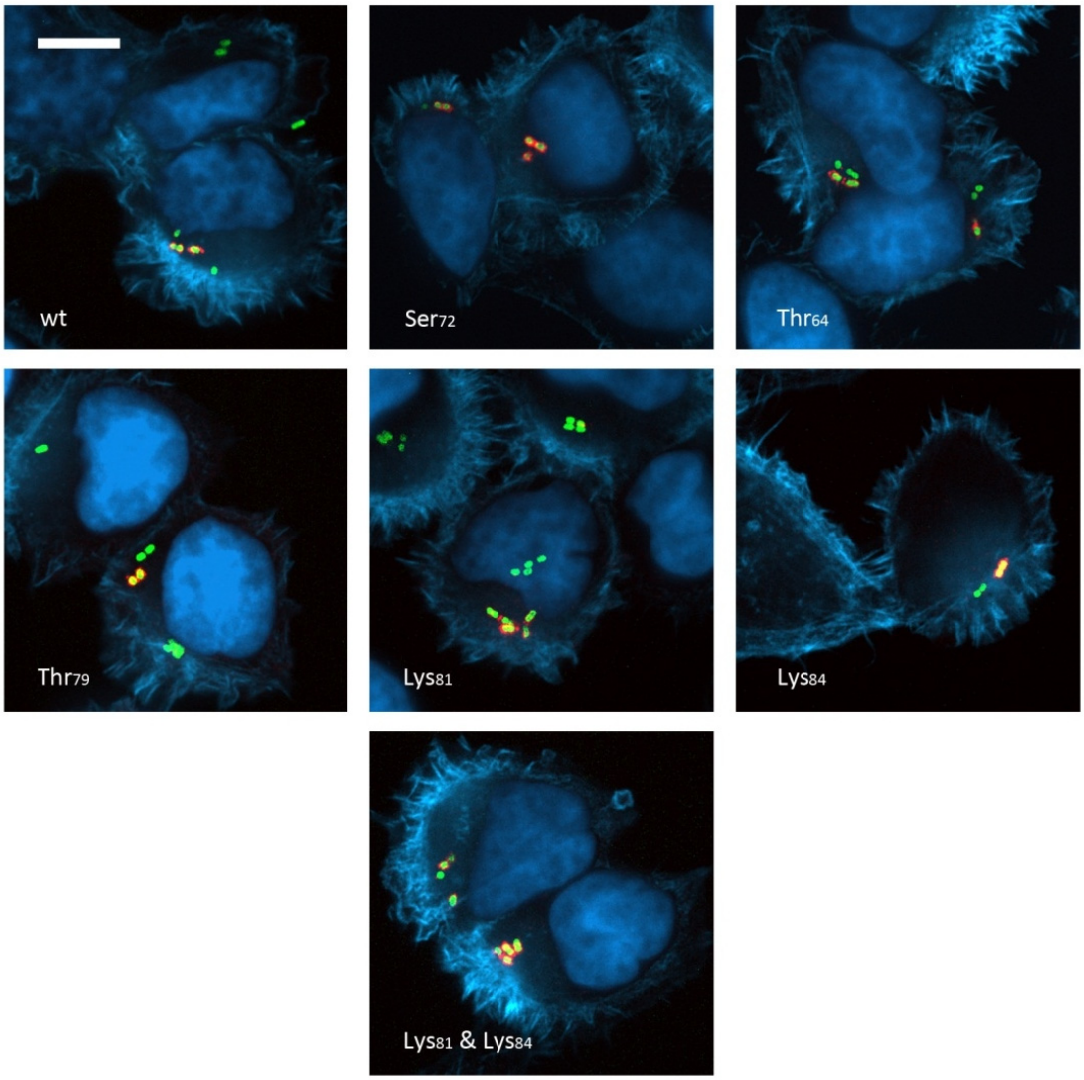

Fig. 3.3 | Single alanine substitutions of SopE do not prevent accumulated SopE around bacteria.
HeLa Kyoto cells were infected with M708 harboring plasmids pM965 and pM438 or the plasmid with the respective amino acid substitution. After 1 h of infection the cells were fixed and processed for immunofluorescence. Image stacks were acquired by fluorescence microscopy. Green: *S.* Tm, red: SopE-M45, light blue: actin cytoskeleton, dark blue: nuclei. Scale bar: 10 µm.

In order to investigate their importance for the localization of SopE, the conserved serines, threonines and lysines were individually substituted for alanines through site-directed mutagenesis, thus generating plasmids $pM438_{T1\text{-}A}$, $pM438_{S\text{-}A}$, $pM438_{T2\text{-}A}$, $pM438_{K1\text{-}A}$ and $pM438_{K2\text{-}A}$ respectively. Furthermore, a plasmid with both lysines substituted for alanines was generated ($pM438_{K1,2\text{-}A}$). HeLa cells were then infected for 1 h with *S*. Typhimurium strain M708 harboring plasmids pM965 and pM438 or one of the modified versions containing the alanine substitutions. Accumulation of visible SopE nearby individual bacteria was observed with all different mutated plasmid versions in fluorescence microscopy (Fig. 3.3).

In order to determine whether the modifications in SopE alter the quantity of protein accumulation or the total amount of SopE inside cells, mean fluorescence intensities were measured over complete cell areas (and normalized to the number of bacteria) or around individual bacteria respectively (Fig. 3.4). No significant differences were observed for the different mutations in comparison to pM438. Strains harboring plasmids $pM438_{K1\text{-}A}$ or $pM438_{K2\text{-}A}$ had slightly higher average values of accumulated SopE around bacteria. Because of relatively high variances however these trends were not found to be significant. Furthermore, *S*. Typhimurium strains infecting with plasmid $pM438_{K1,2\text{-}A}$, which contains alanine substitutions for both lysines residues, had no increased levels of accumulated SopE.

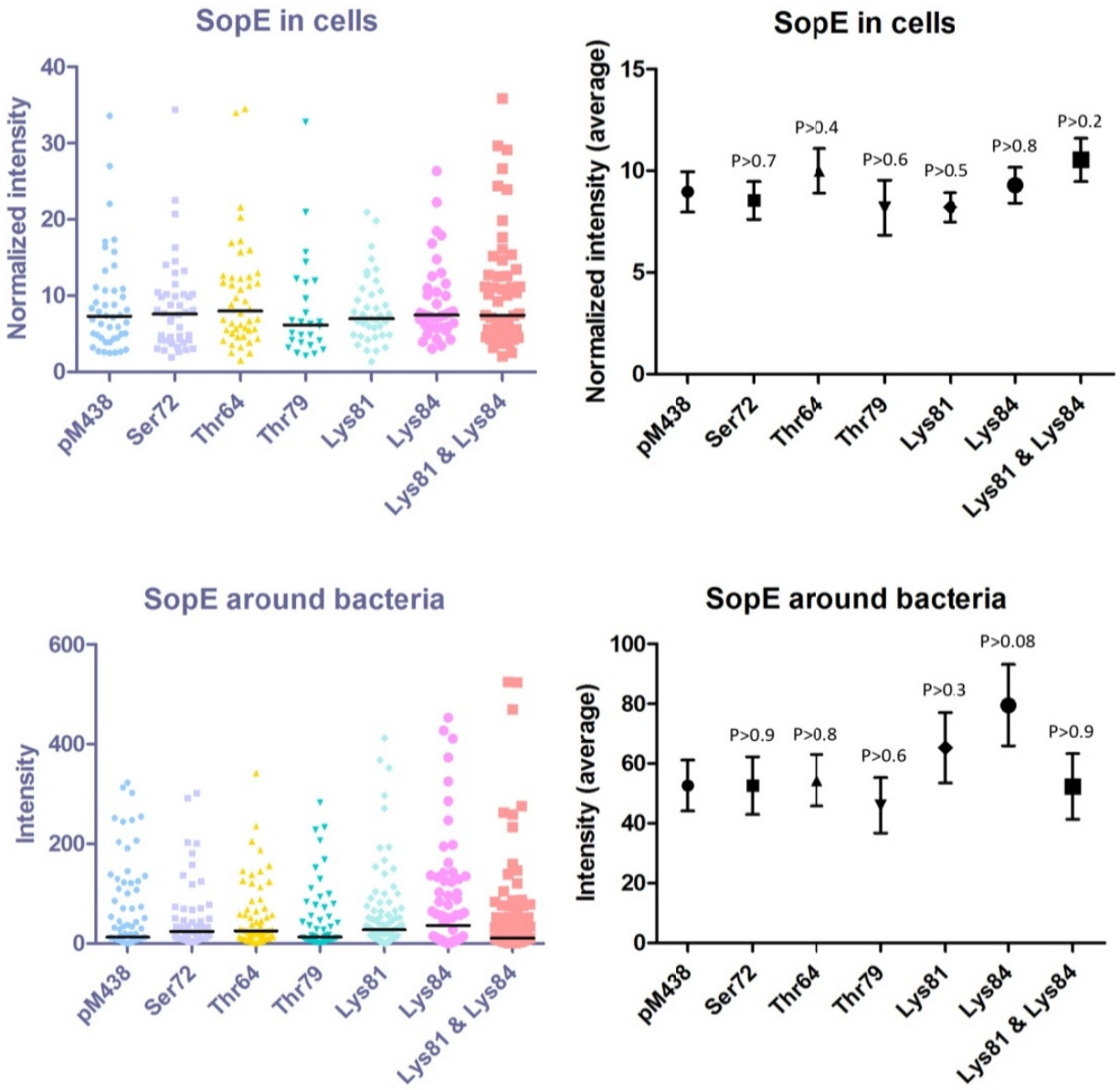

Fig. 3.4 | Substitution of conserved serines, threonines and lysines does not affect SopE accumulation. The intensities of SopE-M45 were measured for whole cells (normalized to the number of bacteria) and around the SCVs. Individual data points (colored) with the median (black line) or average values with standard errors and P values from a t test are plotted.

3.3. Inhibition of ubiquitin-activating enzyme E1

Ubiquitination is a frequent posttranslational modification of eukaryotic proteins. This modification may enable proteins to interact with other proteins that contain an ubiquitin-binding domain. To investigate whether cellular ubiquitination is essential for SopE to accumulate around bacteria, cells were treated with an inhibitor of the ubiquitin-activating enzyme (E1) prior to infection.

The E1 inhibitor used in this experiment (PYR-41) had previously been shown to irreversibly inhibit more than 95% of E1 activity within few hours at a concentration of 50 µmol/l [62]. For this reason, HeLa cells were treated with 50 µmol/l PYR-41 one day prior to infection. In order to verify the functionality of the E1 inhibitor, proteasome inhibitor (MG132) at a concentration of 10 µmol/l was added to some of the cells 20 min prior to infection. Cells were infected with strain M708 harboring plasmids pM965 and pM438.

Both the E1 inhibitor as well as the proteasome inhibitor did not prevent SopE localization to the bacteria (Fig. 3.5, A). For all conditions, accumulated SopE was clearly visible around bacteria. In a next step, fluorescence intensities were compared quantitatively. No significant differences in intensity around bacteria could be determined (Fig. 3.5, B). Comparison of fluorescence intensities within whole cells revealed that degradation of cellular SopE was attenuated in cells that had been treated with proteasomal inhibitor compared to untreated cells. This result was in line with other experiments [18]. However, SopE levels in cells that had been treated with the E1 inhibitor were not significantly different from control cells.

A

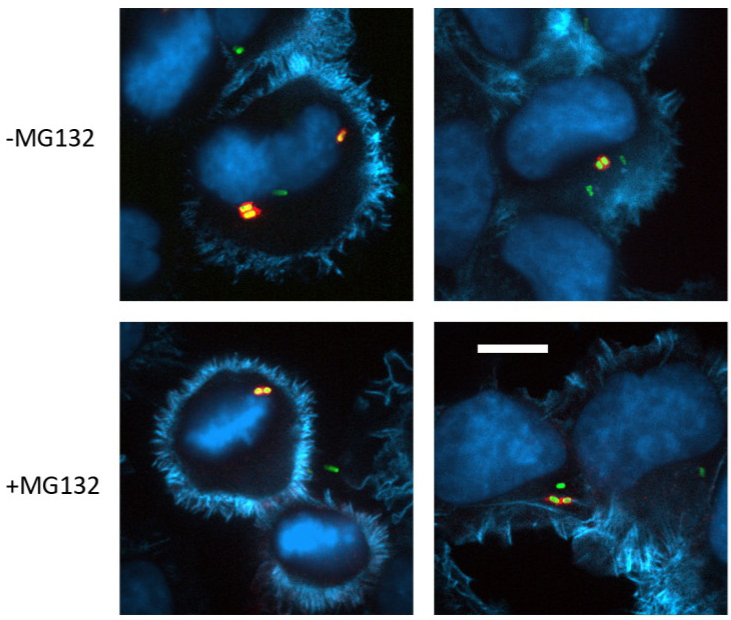
-PYR-41
+PYR-41
-MG132
+MG132

B

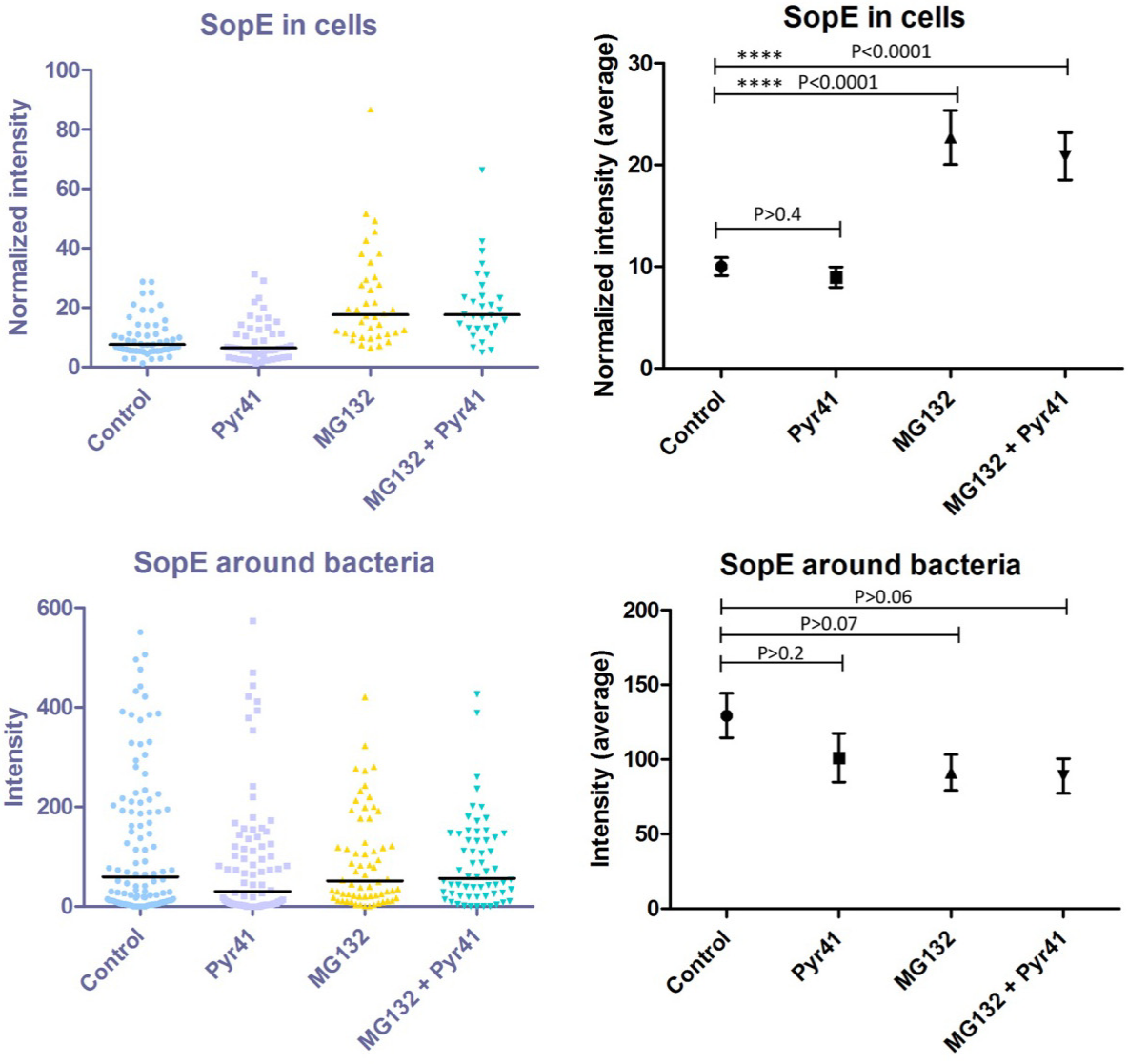
SopE in cells
Normalized intensity
100
80
60
40
20
0
Control
Pyr41
MG132
MG132 + Pyr41
SopE in cells
Normalized intensity (average)
30
20
10
0
**** P<0.0001
**** P<0.0001
P>0.4
Control
Pyr41
MG132
MG132 + Pyr41
SopE around bacteria
Intensity
600
400
200
0
Control
Pyr41
MG132
MG132 + Pyr41
SopE around bacteria
Intensity (average)
200
150
100
50
0
P>0.06
P>0.07
P>0.2
Control
Pyr41
MG132
MG132 + Pyr41

Fig. 3.5 | E1 inhibitor fails to prevent degradation of SopE.
(A) PYR-41 was added to HeLa cells one day prior to infection. MG132 was added 20 min prior to infection. Cells were fixed 1h post infection. Green: *S*. Tm, red: SopE-M45, light blue: actin cytoskeleton, dark blue: nuclei. Scale bar: 10 µm.
(B) The intensities of SopE-M45 were measured for whole cells (normalized to the number of bacteria) and around the SCVs. Individual data points (colored) with the median (black line) or average values with standard errors and P values from a t test are plotted.

3.4. Inhibition of geranylgeranyltransferase I

In order to investigate if geranylgeranylation is involved in the retention of SopE, HeLa cells were treated with 10 µmol/l GGTI one day before infection. GGTI is an inhibitor of GGTase-I, which has been shown to inhibit membrane association of RhoA and Rac1 [63] among others. To check if the inhibitor functioned reliably, a stable HeLa cell line expressing Rac1 fused to GFP was infected with M708 harboring plasmid pM438. Bacteria were stained with an α-LPS primary antibody and an Alexa-647 secondary antibody. Intensity profiles were taken along the surfaces of intracellular bacteria (Fig. 3.6). In cells that had not been treated with GGTI the intensity plots showed increased amounts of SopE and Rac1 on the periphery of the bacteria. In cells that had been treated with the inhibitor however, an accumulation of Rac1 was not detected. For these cells the GFP intensity was rather distributed evenly throughout the cells.
In order to quantify SopE levels, HeLa cells without transfected plasmids were infected with M708 harboring plasmids pM438 and pM965. Cells were fixed and subjected to immunofluorescence staining one hour post infection. Treatment with GGTI did not prevent the accumulation of SopE (Fig. 3.7). No difference in the amounts of accumulated SopE around bacteria was detected between GGTI-treated and untreated cells. When normalized cellular levels of SopE were compared, a decreased amount of injected SopE per bacterium was found in GGTI-treated cells.

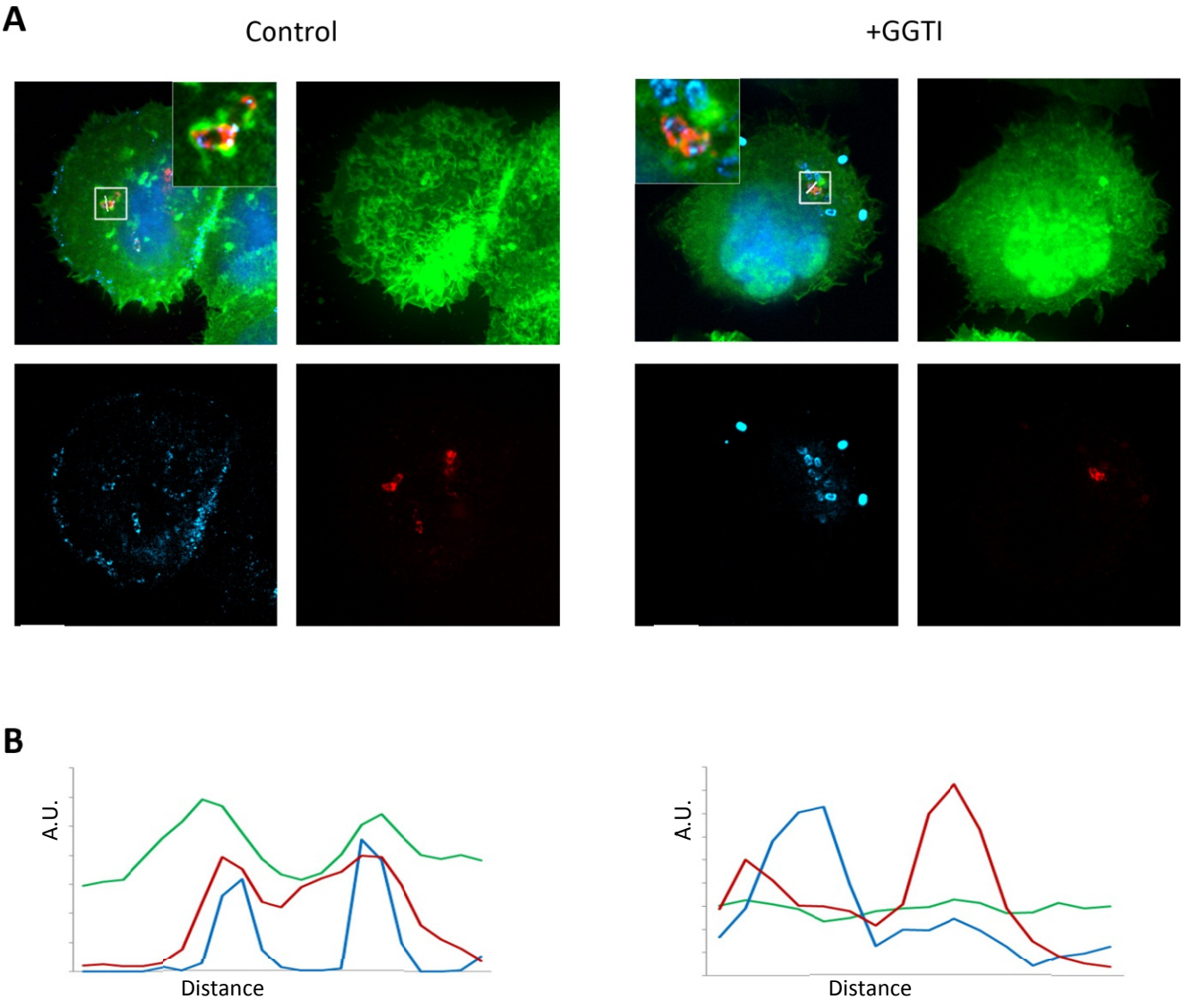

Fig. 3.6 | Treatment with GGTase-I inhibitor GGTI leads to membrane dissociation of Rac1.
(A) Immunofluorescence images of Rac1-GFP transfected HeLa cells which were infected with M708 harboring plasmid pM438 for 1 h. Green: Rac1, red: SopE-M45, light blue: *S*. Tm, dark blue: nuclei. Top left: merge of all channels. Scale bar: 10 µm.
(B) Intensity plots of the profiles indicated in (A). Green: Rac1, red: SopE-M45, blue: *S*. Tm.

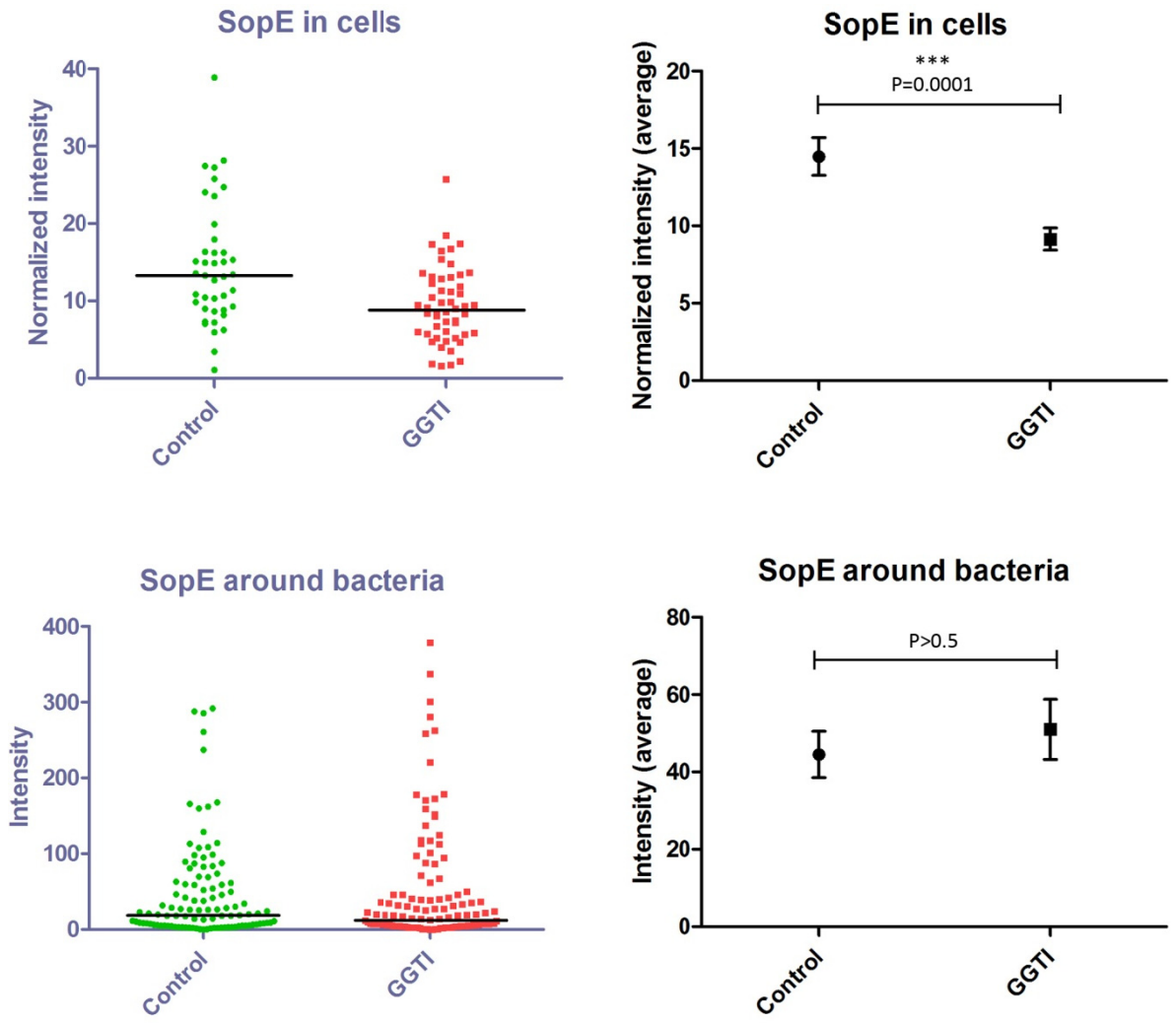

Fig. 3.7 | Treatment with GGTI leads to lower cellular SopE levels but does not affect accumulation at SCVs. The intensities of SopE-M45 were measured for whole cells (normalized to the number of bacteria) and around the SCVs. Individual data points (colored) with the median (black line) or average values with standard errors and P values from a t test are plotted.

3.5. Depletion of small GTPases

The *Salmonella*-containing vacuole is a modified endosome that is associated with various GTPases. To address the question whether small GTPases are required for SopE localization, Rab5c, Rab7a, Cdc42, Rac1, RhoA and RhoG were depleted separately in cells through RNA interference. The efficiency of the interference amounted to roughly 50%, as was determined by monitoring apoptosis in cells depleted for Polo-like kinase (data not shown). As a further control, cells that had been depleted of CopG were included. These cells adopted symmetrical quasi-triangular shapes, as had been seen before [1].

Cells were infected for one hour with *S*. Typhimurium strain M708 harboring plasmids pM965 and pM438 and were prepared for immunofluorescence microscopy. SopE localized to the SCVs in each experiment with depleted GTPases (Fig. 3.8). Quantification of the fluorescence intensities however revealed that bacteria in cells depleted of Rab5c had a higher amount of accumulated SopE (Fig. 3.9). Cells depleted for Cdc42, Rac1, RhoA and RhoG did not show a significant quantitative difference in SopE aggregation compared to control cells. Cellular levels of SopE were higher in Cdc42-depleted cells. Increased cellular amounts were also observed in cells that had been depleted of both Rab5c and Rab7a.

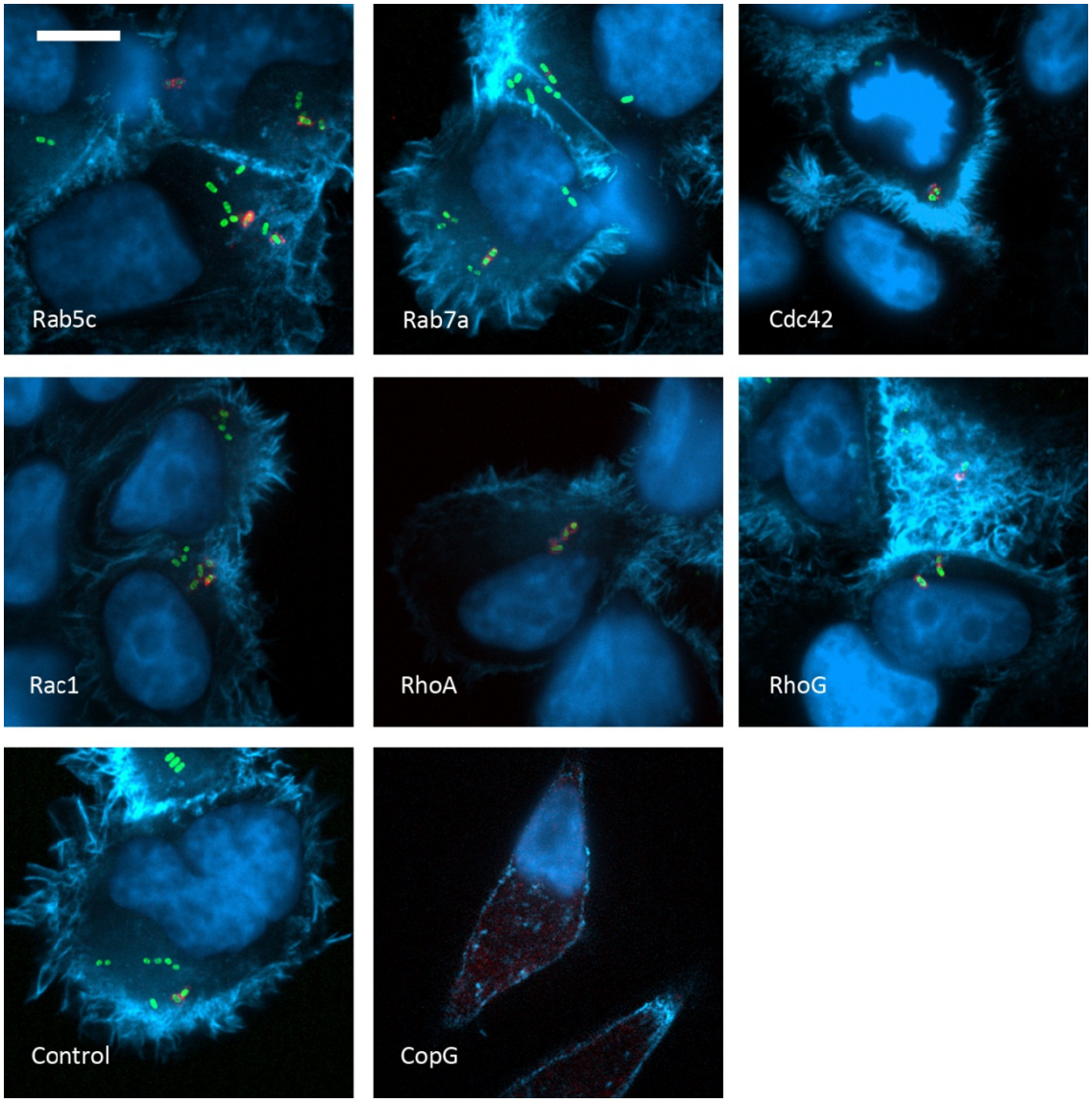

Fig. 3.8 | Depletion of small GTPases does not affect SopE accumulation.
HeLa cells were depleted of various small GTPases and infected for 1 h with strain M708 harboring plasmids pM438 and pM965. Green: *S*. Tm, red: SopE-M45, light blue: actin cytoskeleton, dark blue: nuclei. Scale bar: 10 µm.

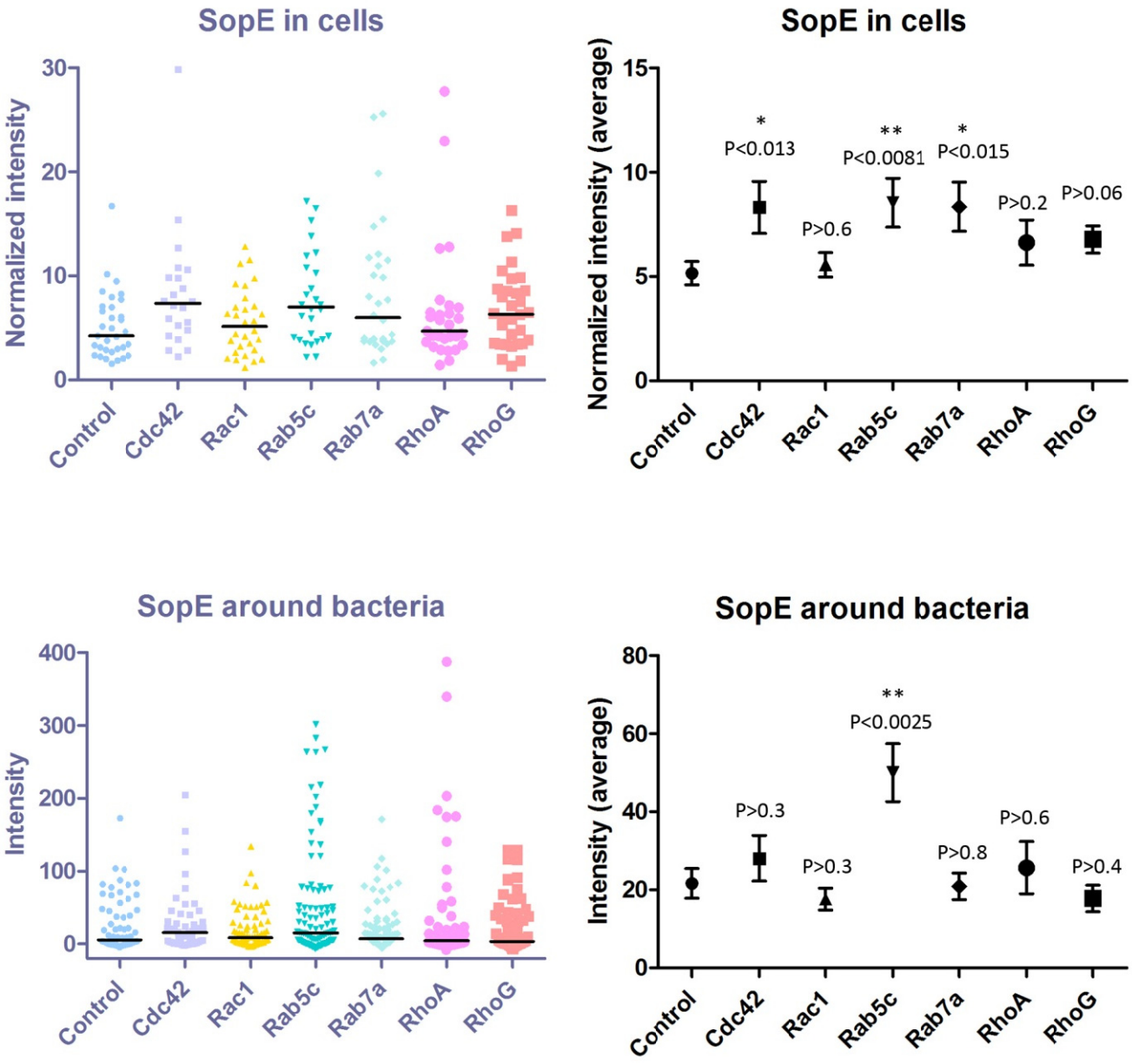

Fig. 3.9 | Depletion of Rab5c leads to increased quantities of SopE-M45 both in whole cells as well as on SCVs. The intensities of SopE-M45 were measured for whole cells (normalized to the number of bacteria) and around the SCVs. Individual data points (colored) with the median (black line) or average values with standard errors and P values from a t test are plotted.

3.6. Inhibition of protein synthesis with chloramphenicol

To address the question whether *S*. Typhimurium continues to produce SopE after internalization into cells, SB875, an *S*. Typhimurium strain that is sensitive to chloramphenicol and has a chromosomally encoded version of SopE that is tagged with the M45 epitope, was used for cell infections. The medium of the cells was supplemented with 30 µg/ml chloramphenicol prior to infection.

Intriguingly, treatment with chloramphenicol completely abrogated accumulation of SopE around bacteria (Fig. 3.10, A). In three independent experiments not a single bacterium with peripherally accumulated SopE was detected, whereas non-treated cells contained several. These observations were confirmed by quantifying fluorescence intensities (Fig. 3.10, B). Bacteria in cells treated with the antibiotic showed minor levels compared to untreated control cells. Yet when cellular amounts of SopE were compared, chloramphenicol-treated cells showed a higher value of SopE per bacterium than control cells.

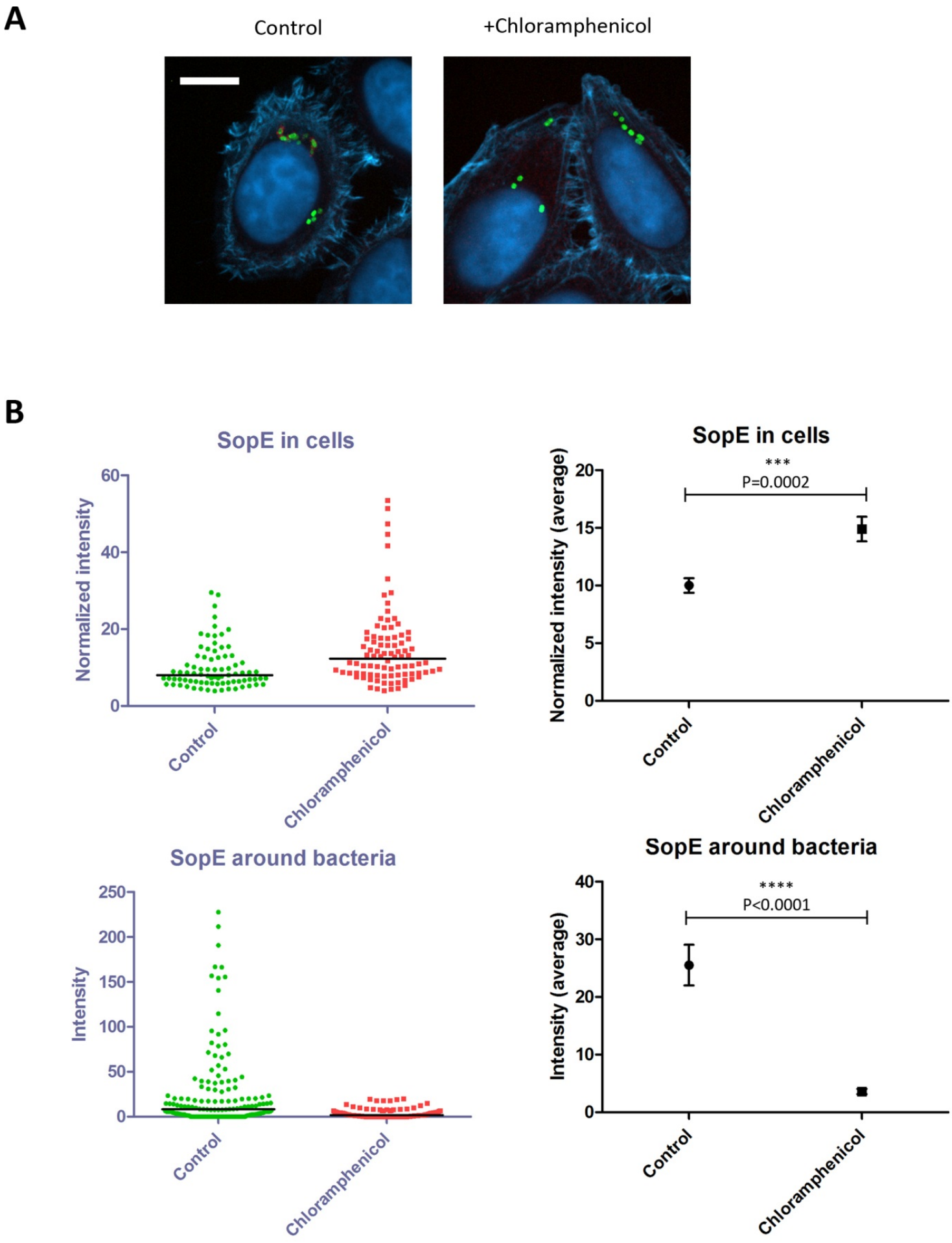
A
Control
+Chloramphenicol
B
SopE in cells
Normalized intensity
60
40
20
0
Control
Chloramphenicol
SopE in cells
***
P=0.0002
Normalized intensity (average)
20
15
10
5
0
Control
Chloramphenicol
SopE around bacteria
Intensity
250
200
150
100
50
0
Control
Chloramphenicol
SopE around bacteria
****
P<0.0001
Intensity (average)
40
30
20
10
0
Control
Chloramphenicol

Fig. 3.10 | Treatment of cells with chloramphenicol prior to infection leads to complete abrogation of SopE association with SCVs.
(A) Immunofluorescence images of HeLa cells that were treated with 30 µg/ml chloramphenicol prior to infection with the chloramphenicol-sensitive *S*. Tm strain SB875 harboring plasmid pM965 for 1 h. Green: *S*. Tm, red: SopE-M45, light blue: actin cytoskeleton, dark blue: nuclei. Scale bar: 10 µm.
(B) The intensities of SopE-M45 were measured for whole cells (normalized to the number of bacteria) and around the SCVs. Individual data points (colored) with the median (black line) or average values with standard errors and P values from a t test are plotted.

3.7. Analysis of SopE-lipid interactions

Another possible mechanism for SopE accumulation around bacteria is the non-covalent binding of the proteins to lipids of the SCV. This hypothesis was tested with membranes that were overcast with 15 different biologically important lipids.

S. Typhimurium strain SB245 was transformed with plasmids pSB1180 (encoding an arabinose-inducible version of SopE containing a Protein A kinase site), pSB1181 (analogous to pSB1180 but additionally fused to M45 epitope) or pM438 (encoding SopE-M45) respectively. Cultures were grown in LB and secreted proteins were concentrated with centrifugation filter devices. SopE from pM438 and pSB1181 was successfully purified (designated SopE-438 and SopE-1181 respectively) whereas bacteria harboring plasmid pSB1180 (SopE-1180) seemed to have lysed in culture since SDS-PAGE of the concentrated supernatant revealed a variety of different bands that looked similar to *Salmonella* whole cell lysates (Fig. 3.11, A). For this reason the extract from this strain was not included in subsequent experiments.

In order to obtain a control for the specificity of a hypothetical SopE-lipid interaction, *E. coli* DH5α was transformed with plasmid pGEX-2TK (encoding GST containing a Protein kinase A site). Cultures were lysed in a French press and GST was purified on a Sepharose 4B column prior to concentration with centrifugation filter devices. Proteins of roughly 45 kDa were co-purified with GST. This band most likely represented a dimer of GST and was not expected to interfere with subsequent experiments. Proteins were phosphorylated with γ-^{32}P-ATP in a reaction with Protein kinase A. Incorporation of radioactive phosphate groups was monitored by measuring radioactivity in an SDS polyacrylamide gel with a Phosphorimager (Fig. 3.11, B). ^{32}P was associated with both SopE-1181 and GST, but not with SopE-438 that lacked a phosphorylation site. Incorporation resulted roughly to the same degree in monomeric GST and SopE-1181 and was most efficient for dimeric GST. The most prominent proportion of ^{32}P had not been incorporated and was present at the gel running front.

In a next step, phosphorylated proteins were incubated on PIP membranes for one hour. Membranes were then washed and exposed to an X-ray film for 22 h in order to determine if proteins were binding. Neither SopE nor GST was found to bind to lipids on the membrane (Fig. 3.11, D). However, since no control reagent with phosphorylation site that binds to lipids was available, the experiment was repeated and proteins were detected with antibodies instead of ^{32}P incorporation. G-4501, a protein specific for $PI(4,5)P_2$, was included as a positive control. G-4501 bound extensively to $PI(4,5)P_2$, indicating that the membranes were intact (Fig. 3.11, E). Neither GST nor SopE-438 or SopE-1181 bound specifically to any lipids. Some signal was present at the periphery of some lipid spots on membranes incubated with SopE. Yet, none of these signals were present over the entire surface of a lipid spot. It is therefore most probable that the signals resulted from unspecific binding of antibodies, indicating that the concentration was too high.

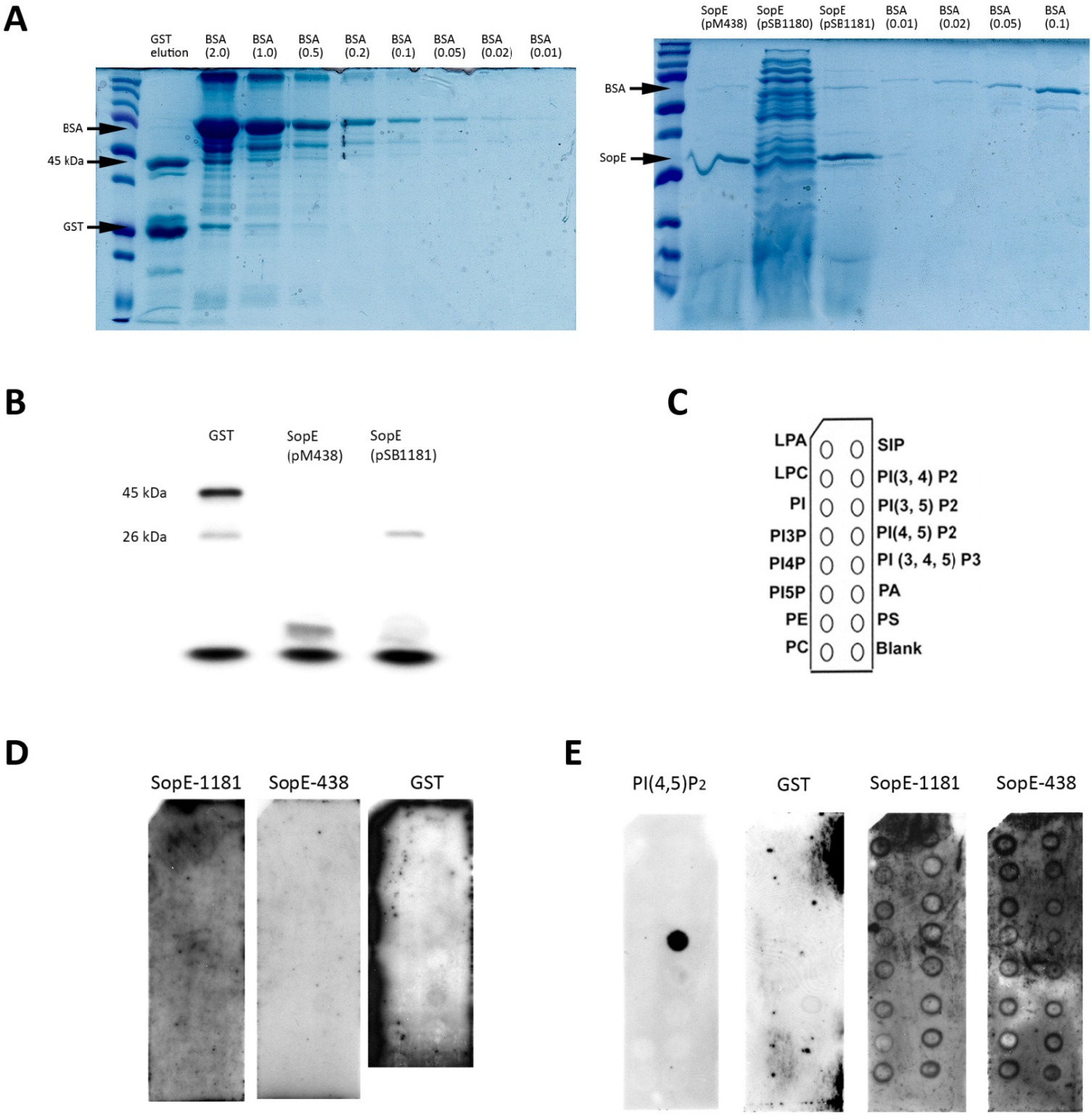

Fig. 3.11 | SopE that was purified from bacterial culture supernatant does not bind to lipids on the PIP membranes. **(A)** Purified proteins were separated on 12% SDS polyacrylamide gels and stained with Coomassie blue. **(B)** Polyacrylamide gel showing separated proteins after phosphorylation reaction with γ-^{32}P-ATP. **(C)** Scheme showing the lipids that are present on the PIP membranes (at 100 pmol). [2] **(D)** Blots of the membranes that were incubated with radioactively labeled proteins and visualized by a Phosphor imager. **(E)** Blots of the membranes that were incubated with the non-phosphorylated proteins. Proteins were detected with antibodies.

3.8. Setting up a protocol for SCV isolation by subcellular fractionation

SopE had previously been found to co-localize with farnesylated GFP (f-GFP) in homogenized cell extracts (P. Vonaesch, personal communication). However, until now there has been no biochemical evidence that SopE actually associates to SCVs. In order to get more insights into the nature of SopE localization to SCVs, a protocol to isolate SCVs was set up. For this purpose HeLa cells were infected with *S*. Typhimurium strain M708 harboring plasmid pM438. After 30 min infection the cells were lysed in a cell homogenizer and a small amount of the homogenate was centrifuged onto a coverslip in order to verify if SopE co-localized with f-GFP. As had been seen before, farnesylated GFP was found to overlap with SopE staining around bacteria (Fig. 3.12, A).

In a next step the homogenate was separated into subcellular fractions by differential centrifugation. After a first, low-speed centrifugation step, non-disrupted cells, bacteria, host cell nuclei and cytoskeletal elements (pellet; fraction P) were separated from the other components. The supernatant was further processed in a high-speed ultracentrifuge and separated into pellets containing membranes (most prominently organelles such as endosomes, lysosomes, mitochondria and peroxisomes; fraction M) and supernatants with cytoplasmic proteins and fragments from plasma membranes and endoplasmic reticulum (fraction C).

Furthermore, in order to determine the nature of a possible interaction of SopE with membranes, the pellets of fraction M were resuspended in Tris buffer containing 0.15 M NaCl (M1), 1 M NaCl (M2), 0.1 M sodium carbonate at pH 11.5 (without Tris; M3) or 1% Triton X-100 (M4). A similar experiment had been carried out earlier with the effector protein SopB, which also localizes peripherally around intracellular *Salmonella* [46]. Treatment of the membrane fraction with high salt (1 M NaCl) disrupts hydrophilic protein interactions while treatment with a buffer of high pH abolishes hydrophobic interactions and releases soluble proteins within the vesicles [46]. Treatment with Triton X-100 solubilizes integral membrane proteins. After centrifugation, proteins from the supernatants were precipitated with trichloroacetic acid. Pellets (p), precipitated proteins from supernatants (s) and an *S*. Tm overnight culture were resuspended in Lämmli sample buffer, separated by SDS-PAGE and assayed for SopE-M45 with Western blot analysis. In order to check the purity of the isolation, fractions P, C and M were additionally assayed for the presence of the lysosomal glycoprotein Lamp1 and of LPS.

LPS was detected in fraction P as well as in bacterial overnight cultures (Fig. 3.12, B). SopE-M45 was only present in the lanes with overnight cultures but not in fractions that had been isolated from the homogenized cells (Fig. 3.12, C). Furthermore, Lamp1 was not detected in any of the fractions.

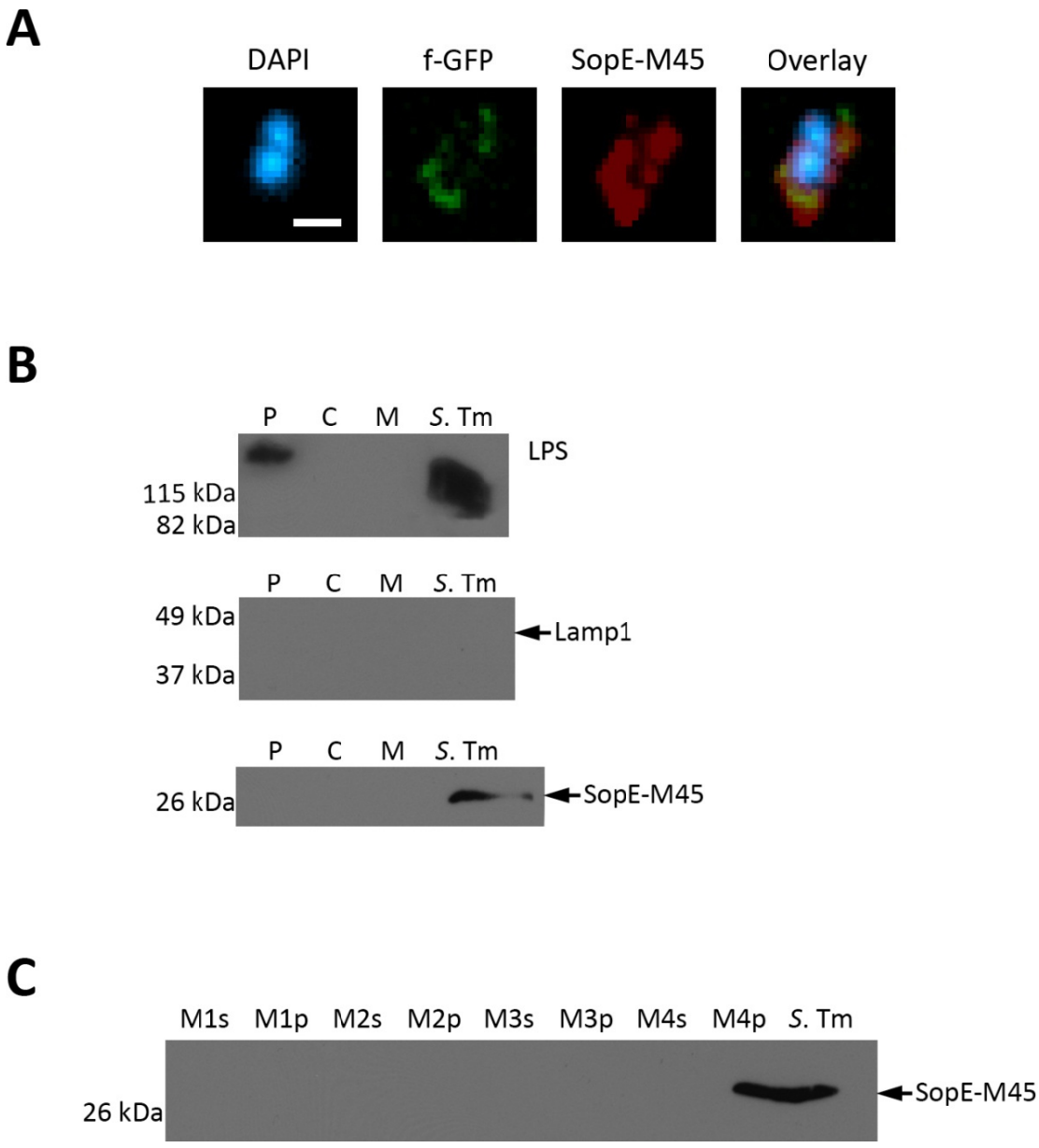

Fig. 3.12 | Lamp1 and SopE-M45 are not detected in the fractions.
(A) Immunofluorescence images showing the co-localization of SopE-M45 with SCVs after disrupting plasma membranes in a cell homogenizer. Green: f-GFP, red: SopE-M45, blue: *S*. Tm. Scale bar: 1 µm. **(B)** Western blot analysis of fractions containing low-speed centrifugation pellet (P), high-speed centrifugation pellet (M), supernatant (C) or a lysed *S*. Tm culture, probed for LPS, Lamp-1 and SopE-M45. **(C)** Western blot analysis of the membrane fraction supernatants (s) or pellets (p) that were treated with 0.15 M NaCl (1), 1 M NaCl (2), 0.1 M sodium carbonate at pH 11.5 (3) or 1% Triton X-100 (4).

3.9. Time-lapse microscopy with red bacteria

No plasmid encoding a red fluorescent protein has been successfully established for infection during time-lapse microscopy. It would be highly helpful to have such a red bacterial marker since most plasmids used for cell transfection that encode recombinant proteins are coupled to GFP. For this reason, *S*. Tm strains M708 harboring plasmid pM438 were transformed individually with four different plasmids encoding versions of *Discosoma* sp. red fluorescent protein (dsRed) or mCherry. Kyoto cells were seeded into glass-bottom dishes, buffered with HEPES and put into a specimen holder of a confocal microscope that had been pre-warmed to 35°C. This procedure had been established earlier for real-time infection with *S*. Typhimurium [58]. Cells were infected directly while being observed under the microscope. Time-lapse images were recorded in order to analyze both the red appearance of bacteria and the capacity to invade cells with each different plasmid.

Bacteria encoding versions of dsRed were not detectable in the red channel, even with exposure times of more than 2 seconds (Fig. 3.13). Bacteria harboring plasmid pM2120 (encoding mCherry) on the other hand were quite well visible. As observed in the bright field channel there were however two subpopulations of these bacteria: one that expressed mCherry and one that didn't. *S*. Tm expressing the fluorescent protein were not found to induce cell ruffling whereas the subpopulation that didn't express it induced large ruffles. Therefore it has to be assumed that the bacteria that synthesized mCherry were heavily attenuated in their invasion potential.

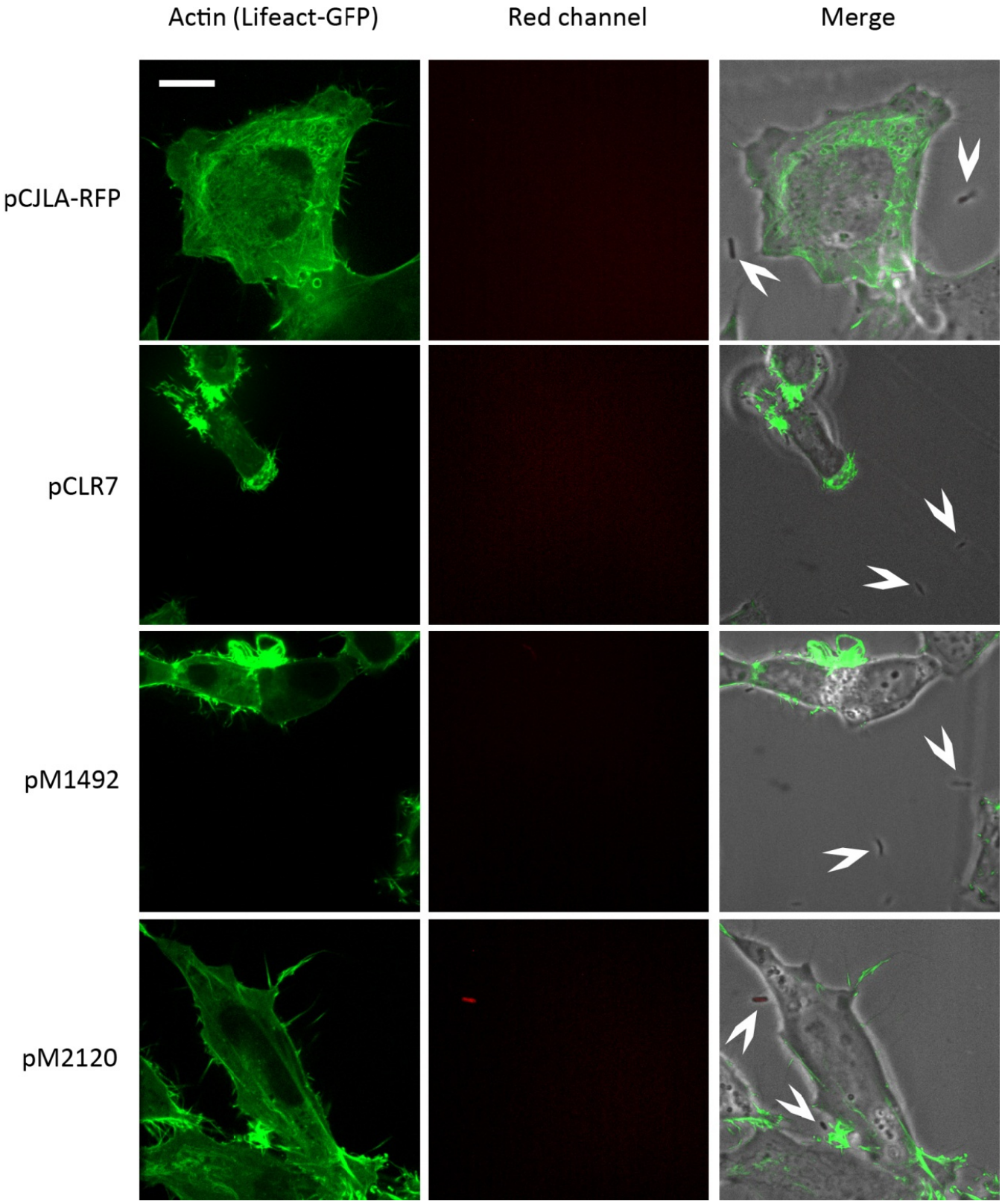

Fig. 3.13 | mCherry fluorescent protein is visible in time-lapse microscopy but attenuates virulence. Images showing single time frames of time-lapse microscopy with Lifeact-GFP transfected HeLa cells and an *S*. Tm strain harboring different plasmids for constitutive expression of red fluorophores. Green: actin, red: *S*. Tm. Right column: Merged fluorescence channels with the bright field channel. Scale bar: 10 µm.

4. Discussion

In this study several approaches were followed to investigate the nature of SopE interaction with the SCV. The first experiments investigated whether some kinds of posttranslational modifications of SopE were involved in the localization to SCVs. It is thought that such modifications occur in a variety of bacterial effector proteins and that some of these might be responsible for the "anchoring" of effectors to membranes [64]. In subsequent experiments the questions whether SopE binds directly to lipids and if it is continuously translocated within host cells were addressed.

4.1. Conserved Ser, Thr and Lys seem not to be involved in SopE localization

A truncated version of SopE containing only the first 100 amino acids was previously found to be sufficient for intracellular accumulation of SopE around bacteria. Infection with an *S*. Typhimurium strain that encoded only the first 60 amino acids of SopE however yielded no observable localization to SCVs anymore [39]. These findings indicate that a sequence that is responsible for the localization of the protein might be present in the region between amino acids 60 and 100. Furthermore, since SopE2, a close homologue of SopE, also accumulates around bacteria after infection [39] it is possible that this process is mediated by one or a few amino acids that are conserved between both proteins. Alignment of the two proteins identified two conserved lysines within this region. Additionally a conserved serine and two conserved threonines were found. Since these amino acids might be targets of ubiquitination or phosphorylation respectively they were individually substituted for alanines in this study. However, neither the single knockout mutants nor a version of SopE with both lysines substituted for alanines ceased to localize around bacteria. These data indicate that none of these conserved amino acids alone promote the interaction of SopE with SCVs. Additionally, since the cellular levels of SopE did not significantly vary between the lysine mutants and the wildtype, it can be concluded that the proteasomal degradation of SopE is neither dependent on Lys_{81} nor on Lys_{84}.

A good control to investigate whether ubiquitination is indeed not involved in SopE localization to SCVs would have been to inhibit the process of ubiquitination in cells. However, treatment of cells with PYR-41 did not result in higher cellular levels of SopE compared to untreated cells. This was contrary to the expectations since SopE is thought to be degraded in the proteasome and the function of E1 is to block the ubiquitination of proteins, which is an indispensable first

step to target proteins to the proteasome. For this reason it has to be assumed that the inhibitor did not prevent ubiquitination properly.

4.2. Geranylgeranylation by GGTase-I is not required for SopE localization

Several mammalian GTPases rely on posttranslational prenylation for their association with membranes (see section 1.3). In this process, enzymes couple either a farnesyl (15 carbon atoms) or a geranylgeranyl (20 carbon atoms) lipid moiety to a cysteine residue located at the C-terminus of the protein. In this study GGTI was used to inhibit GGTase-I. The amount of accumulated SopE around bacteria was not found to be significantly different in GGTI-treated cells than in untreated cells. These data indicate that (i) the presence of geranylgeranylated Rho GTPases at the SCV is not required for SopE localization and (ii) SopE is not itself modified by GGTase-I in order to relocate to SCVs. However, cellular levels of SopE were found to be lower in cells that had been treated with GGTI compared to untreated cells. At first glance, these results may be counterintuitive. Interestingly it has been found for *Yersinia pseudotuberculosis* that efficient translocation of effector proteins correlates with the activation of cellular Rho GTPases [65]. It is possible that Rho GTPases also influence the efficient translocation of *S*. Typhimurium effector proteins. This would provide an explanation for the lower levels of SopE observed with the GGTI-treated cells, where no active Rho GTPases are expected to be present at membranes.

On the other hand depletion of Rab5c, Rab7a and the Rho GTPase Cdc42 resulted in higher cellular levels of SopE, whereas depletion of Rac1, RhoA and RhoG had no effect. These data seem to contradict the results obtained for GGTI-treated cells. Yet, it has to be kept in mind that treatment with GGTI inhibits GGTase-I, which results in depletion of all of its substrates at the same time. It is therefore difficult to compare both experiments. Additionally, the experiment with depleted GTPases was only performed once due to a lack of siRNA and there was no control for the efficiencies of the individual depletions. Thus it has to be taken care with the interpretation of these results. Nevertheless the data obtained for Rab5c depletion, where both cellular as well as SCV-accumulated concentrations of SopE were significantly higher than in control cells, seem interesting. A previous study demonstrated that SopE that localizes around SCVs is able to retain non-prenylated Rab5 at SCVs [38]. One can imagine that upon inhibition of GGTase-I and thus depletion of membrane-bound Rab5, *S*. Typhimurium needs to translocate increased amounts of SopE in order to recruit sufficient Rab5 GTPases for efficient vesicle trafficking and SCV maturation. Is it possible that some kind of feedback loop is involved in the regulation of SopE translocation? Further investigation in this direction is needed in order

to verify if depletion of Rab5c indeed leads to higher levels of SopE, and if so, to gain more insights into the mechanisms involved.

4.3. Further possibilities for SopE interaction

A variety of proteins bind directly to membrane lipids. To address the question whether SopE is one of these, the effector protein was purified from *S*. Typhimurium cultures and assayed for binding on PIP membranes in this study. No direct interaction between SopE and any of the lipids present on the membranes was found. There are however a few limitations to this experiment. First, any hypothetical posttranslational modifications of the protein were prohibited since it was purified directly from bacterial supernatant. This experiment was designed to investigate only whether secreted, unmodified SopE binds to lipids. Secondly, the lipids on the PIP membranes may be in a different conformation than in cultured cells. For these reasons it cannot be definitely ruled out that SopE binds to lipids, yet the experiment provides some arguments against it.

In order to confirm the binding of SopE to SCVs, the elaboration of a protocol for the isolation of SCVs from infected HeLa cells has been initiated in this study. Furthermore, possibilities to determine the nature of the interaction by treatment of the membrane fractions with different reagents are proposed. At the moment this protocol is not yet fully elaborated. One limitation of the protocol is that it is not clear whether the number of cells used for infection is sufficient for the detection of markers by Western blot analysis. A second issue concerns the precipitation of proteins from supernatants with trichloroacetic acid. The precipitation results in dense pellets, which are hard to re-suspend and hence a lot of proteins may remain in the pellets. Treatment with a basic compound could possibly facilitate the re-dissolving of proteins and can be included in the protocol. Additionally the protocol can be improved by including proteasome inhibitor MG132 in the cell culture medium to prevent rapid degradation of SopE. If protein levels are still too low for detection, infection of non-adherent cells that grow much denser than adherent cells could be tested. In any case it would be helpful to have some biochemical evidence that there is an interaction of SopE with SCVs.

Another interesting question that remains to be answered is to which side of the SCV SopE actually localizes. It was determined earlier for SipA that it is present at the cytoplasmic face of the SCV [47] and it is probable that the same holds true for SopE. Nevertheless future studies will have to address this question and one way to do this is to follow infections of cells expressing fluorescently labeled chaperone InvB with time-lapse microscopy. Before setting up

the protocol however bacteria with a plasmid encoding a red fluorescent protein that is readily detectable in time-lapse microscopy and doesn't attenuate the virulence are required.

4.4. Chloramphenicol treatment abrogates localization to SCVs

A previous study investigated if SopE is continuously synthesized and translocated after invasion [39]. The question was addressed by treating the cells with chloramphenicol and quantifying the amount of SopE around bacteria. A major limitation of the experimental procedure however was that the *S*. Tm strain used for infection encoded a chloramphenicol acetyltransferase, which rendered it resistant to the antibiotic. For this reason the experiment was repeated with a strain that encoded SopE-M45 on the chromosome and was not resistant to chloramphenicol. Treatment with chloramphenicol inhibited SopE localization to SCVs completely. An obvious explanation for this observation is that SopE continues to be synthesized after invasion and SopE that localizes around SCVs is freshly translocated by *S*. Typhimurium from within SCVs. Yet, the cellular levels of SopE were found to be significantly higher in cells treated with chloramphenicol than in untreated ones. This difference may be misleading and due to some fluorescent properties of chloramphenicol itself.

An alternative explanation for these results may be that SopE that accumulates around bacteria is not newly translocated from within the SCVs but rather originates from cytoplasmic SopE that re-localizes to the vacuoles. In this case the difference in SopE concentrations between chloramphenicol-treated and untreated cells could be explained by the interference of the antibiotic with the redistribution of the effector protein in a yet unknown mechanism.

To get more insights into these questions, a protocol with erythromycin, a different inhibitor of bacterial protein synthesis, was set up (not shown in this study). *S*. Typhimurium was however resistant to the antibiotic as it failed to inhibit growth of the bacteria. Indeed, several Gram-negative bacteria seem to have a low susceptibility to erythromycin compared to Gram-positive bacteria [66]. Previous experiments found that a pretreatment of various cultures of Gram-negative bacteria (including *Salmonella*) lead to increased susceptibility to the antibiotic [66]. However, these findings could not be replicated for *S*. Tm in this study (data not shown).

An additional possibility to address the above-mentioned questions would be to engineer an *S*. Typhimurium strain that encodes SopE under the control of a promoter that is repressed upon cell invasion. For example, a construct with the lac promoter or the arabinose-inducible p_{BAD} could be tested. Moreover, a more sophisticated experimental setup would be to have a promoter that is repressed by a polypeptide that, in turn, is expressed under the control of a SPI-2 promoter. Since SPI-2 expression is initiated only upon invasion, the repressor of SopE

would inhibit the expression of the effector within cells. The results of such experiments could exclude the hypothetical contribution of chloramphenicol to the measured fluorescence intensities and serve as powerful controls to determine whether SopE at the SCVs is newly translocated or results from a redistribution of SopE from within the cytoplasm.

4.5. Conclusions

In the past decade indications for a secondary role of TTSS-1-translocated *Salmonella* effector proteins have started to emerge [49]. In addition to their function in bacterial invasion, SopB, SopE, SopE2 and SipA have all been found to accumulate around *Salmonella*-containing vacuoles [39, 46, 47]. Furthermore, *S*. Typhimurium strains lacking the effector protein SipA [47], SopE or SopE2 (P. Vonaesch, personal communication) show remarkable deficiencies in their abilities of intracellular replication. This suggests that SPI-2 does not coordinate the intracellular maturation of SCVs on its own but does additionally rely on effectors that are translocated by TTSS-1. With respect to these findings it is reasonable to propose that SopE translocation is not stopped after cell invasion. Similar observations of continued translocation of SipA and SopB further support this hypothesis [46, 47]. It remains an interesting task to investigate the precise functions of SopE during the maturation of SCVs and to use other approaches in order to investigate the mechanisms that lead to the localization of SopE to SCVs.

5. Acknowledgements

I thank Prof. Wolf-Dietrich Hardt for giving me the possibility to do research in his group and for giving me valuable advice. On this occasion I also want to thank Prof. Annette Oxenius for accepting to be the co-referee of my Master thesis.
Pascale, my supervisor during the Master thesis, has accompanied me very enthusiastically and competently through the very diverse experiments I have performed. I have really learned a lot during that time and want to thank her for all her dedicated support and the interesting discussions we had.
Furthermore I want to thank Helge Abicht for advices on subcellular fractionation, Markus Schlumberger for sharing his experiences with time-lapse microscopy, Mikael for improving the situation with the cell incubators and for valuable discussions, Alex for teaching me how to "disrupt" bacteria and for keeping (law and) order in the lab, Carmen, Bala and Tsuyoshi for their help with molecular cloning techniques, and all the people of the research group for interesting discussions, good company and a great atmosphere.
Prof. Hans-Martin Fischer has been very helpful with his introductions to working with radioactive material and the use of the Phosphorimager as well as the ultracentrifuge and I want to thank him very much for his help. Last but no least I want to thank all the people who enormously facilitate research in the institute, especially Daniel, Palmira, Olympia, Susanne and the IT staff.

6. References

1. Misselwitz, B., et al., *RNAi screen of Salmonella invasion shows role of COPI in membrane targeting of cholesterol and Cdc42.* Mol Syst Biol, 2011. **7**: p. 474.
2. Vijayasarathy, C., et al., *Retinoschisin is a peripheral membrane protein with affinity for anionic phospholipids and affected by divalent cations.* Invest Ophthalmol Vis Sci, 2007. **48**(3): p. 991-1000.
3. *Reorganizing the protein space at the Universal Protein Resource (UniProt).* Nucleic Acids Res, 2012. **40**(Database issue): p. D71-5.
4. Cornelis, G.R., *The type III secretion injectisome.* Nat Rev Microbiol, 2006. **4**(11): p. 811-25.
5. Goley, E.D. and M.D. Welch, *The ARP2/3 complex: an actin nucleator comes of age.* Nat Rev Mol Cell Biol, 2006. **7**(10): p. 713-26.
6. McQuiston, J.R., et al., *Molecular phylogeny of the salmonellae: relationships among Salmonella species and subspecies determined from four housekeeping genes and evidence of lateral gene transfer events.* J Bacteriol, 2008. **190**(21): p. 7060-7.
7. Gruenheid, S. and B.B. Finlay, *Microbial pathogenesis and cytoskeletal function.* Nature, 2003. **422**(6933): p. 775-81.
8. Hahn, H., et al., *Medizinische Mikrobiologie und Infektiologie*. 6th ed2009: Springer.
9. Qin, J., et al., *A human gut microbial gene catalogue established by metagenomic sequencing.* Nature, 2010. **464**(7285): p. 59-65.
10. Stecher, B. and W.D. Hardt, *Mechanisms controlling pathogen colonization of the gut.* Curr Opin Microbiol, 2011. **14**(1): p. 82-91.
11. Doolittle, R.F., et al., *Determining divergence times of the major kingdoms of living organisms with a protein clock.* Science, 1996. **271**(5248): p. 470-7.
12. Todar, K. *Salmonella and Salmonellosis in Todar's online textbook of bacteriology.* 2005 [cited 2012; Available from: http://textbookofbacteriology.net/salmonella.html.
13. Sanchez-Vargas, F.M., M.A. Abu-El-Haija, and O.G. Gomez-Duarte, *Salmonella infections: an update on epidemiology, management, and prevention.* Travel Med Infect Dis, 2011. **9**(6): p. 263-77.
14. Worrall, L.J., E. Lameignere, and N.C. Strynadka, *Structural overview of the bacterial injectisome.* Curr Opin Microbiol, 2011. **14**(1): p. 3-8.
15. Lara-Tejero, M. and J.E. Galan, *Salmonella enterica serovar typhimurium pathogenicity island 1-encoded type III secretion system translocases mediate intimate attachment to nonphagocytic cells.* Infect Immun, 2009. **77**(7): p. 2635-42.
16. Cornelis, G.R., *Yersinia type III secretion: send in the effectors.* J Cell Biol, 2002. **158**(3): p. 401-8.
17. Hautefort, I., M.J. Proenca, and J.C. Hinton, *Single-copy green fluorescent protein gene fusions allow accurate measurement of Salmonella gene expression in vitro and during infection of mammalian cells.* Appl Environ Microbiol, 2003. **69**(12): p. 7480-91.
18. Galan, J.E., *Salmonella interactions with host cells: type III secretion at work.* Annu Rev Cell Dev Biol, 2001. **17**: p. 53-86.
19. Wennerberg, K., K.L. Rossman, and C.J. Der, *The Ras superfamily at a glance.* J Cell Sci, 2005. **118**(Pt 5): p. 843-6.
20. Vetter, I.R. and A. Wittinghofer, *The guanine nucleotide-binding switch in three dimensions.* Science, 2001. **294**(5545): p. 1299-304.
21. Schmidt, A. and A. Hall, *Guanine nucleotide exchange factors for Rho GTPases: turning on the switch.* Genes Dev, 2002. **16**(13): p. 1587-609.

22. Bernards, A. and J. Settleman, *GAP control: regulating the regulators of small GTPases.* Trends Cell Biol, 2004. **14**(7): p. 377-85.
23. Kozma, R., et al., *The Ras-related protein Cdc42Hs and bradykinin promote formation of peripheral actin microspikes and filopodia in Swiss 3T3 fibroblasts.* Mol Cell Biol, 1995. **15**(4): p. 1942-52.
24. Heasman, S.J. and A.J. Ridley, *Mammalian Rho GTPases: new insights into their functions from in vivo studies.* Nat Rev Mol Cell Biol, 2008. **9**(9): p. 690-701.
25. Jaffe, A.B. and A. Hall, *Rho GTPases: biochemistry and biology.* Annu Rev Cell Dev Biol, 2005. **21**: p. 247-69.
26. Zhou, D., M.S. Mooseker, and J.E. Galan, *Role of the S. typhimurium actin-binding protein SipA in bacterial internalization.* Science, 1999. **283**(5410): p. 2092-5.
27. McGhie, E.J., R.D. Hayward, and V. Koronakis, *Cooperation between actin-binding proteins of invasive Salmonella: SipA potentiates SipC nucleation and bundling of actin.* EMBO J, 2001. **20**(9): p. 2131-9.
28. Lilic, M., et al., *Salmonella SipA polymerizes actin by stapling filaments with nonglobular protein arms.* Science, 2003. **301**(5641): p. 1918-21.
29. Hardt, W.D., et al., *S. typhimurium encodes an activator of Rho GTPases that induces membrane ruffling and nuclear responses in host cells.* Cell, 1998. **93**(5): p. 815-26.
30. Schlumberger, M.C. and W.D. Hardt, *Salmonella type III secretion effectors: pulling the host cell's strings.* Curr Opin Microbiol, 2006. **9**(1): p. 46-54.
31. Hall, A., *Rho GTPases and the control of cell behaviour.* Biochem Soc Trans, 2005. **33**(Pt 5): p. 891-5.
32. Zhou, D., et al., *A Salmonella inositol polyphosphatase acts in conjunction with other bacterial effectors to promote host cell actin cytoskeleton rearrangements and bacterial internalization.* Mol Microbiol, 2001. **39**(2): p. 248-59.
33. Fu, Y. and J.E. Galan, *A salmonella protein antagonizes Rac-1 and Cdc42 to mediate host-cell recovery after bacterial invasion.* Nature, 1999. **401**(6750): p. 293-7.
34. Ehrbar, K., B. Winnen, and W.D. Hardt, *The chaperone binding domain of SopE inhibits transport via flagellar and SPI-1 TTSS in the absence of InvB.* Mol Microbiol, 2006. **59**(1): p. 248-64.
35. Karavolos, M.H., et al., *Type III secretion of the Salmonella effector protein SopE is mediated via an N-terminal amino acid signal and not an mRNA sequence.* J Bacteriol, 2005. **187**(5): p. 1559-67.
36. Mirold, S., et al., *Isolation of a temperate bacteriophage encoding the type III effector protein SopE from an epidemic Salmonella typhimurium strain.* Proc Natl Acad Sci U S A, 1999. **96**(17): p. 9845-50.
37. Kubori, T. and J.E. Galan, *Temporal regulation of salmonella virulence effector function by proteasome-dependent protein degradation.* Cell, 2003. **115**(3): p. 333-42.
38. Mukherjee, K., et al., *SopE acts as an Rab5-specific nucleotide exchange factor and recruits non-prenylated Rab5 on Salmonella-containing phagosomes to promote fusion with early endosomes.* J Biol Chem, 2001. **276**(26): p. 23607-15.
39. Singh, V., *Intracellular localization of SopE and SopE2 in the host cells upon infection by Salmonella Typhimurium.*, in *Master thesis*2011, ETH Zurich.
40. Steele-Mortimer, O., *The Salmonella-containing vacuole: moving with the times.* Curr Opin Microbiol, 2008. **11**(1): p. 38-45.
41. Abrahams, G.L., P. Muller, and M. Hensel, *Functional dissection of SseF, a type III effector protein involved in positioning the salmonella-containing vacuole.* Traffic, 2006. **7**(8): p. 950-65.

42. Brumell, J.H., et al., *Characterization of Salmonella-induced filaments (Sifs) reveals a delayed interaction between Salmonella-containing vacuoles and late endocytic compartments.* Traffic, 2001. **2**(9): p. 643-53.
43. Rathman, M., M.D. Sjaastad, and S. Falkow, *Acidification of phagosomes containing Salmonella typhimurium in murine macrophages.* Infect Immun, 1996. **64**(7): p. 2765-73.
44. Garcia-del Portillo, F. and B.B. Finlay, *Targeting of Salmonella typhimurium to vesicles containing lysosomal membrane glycoproteins bypasses compartments with mannose 6-phosphate receptors.* J Cell Biol, 1995. **129**(1): p. 81-97.
45. Stein, M.A., et al., *Identification of a Salmonella virulence gene required for formation of filamentous structures containing lysosomal membrane glycoproteins within epithelial cells.* Mol Microbiol, 1996. **20**(1): p. 151-64.
46. Marcus, S.L., L.A. Knodler, and B.B. Finlay, *Salmonella enterica serovar Typhimurium effector SigD/SopB is membrane-associated and ubiquitinated inside host cells.* Cell Microbiol, 2002. **4**(7): p. 435-46.
47. Brawn, L.C., R.D. Hayward, and V. Koronakis, *Salmonella SPI1 effector SipA persists after entry and cooperates with a SPI2 effector to regulate phagosome maturation and intracellular replication.* Cell Host Microbe, 2007. **1**(1): p. 63-75.
48. Madan, R., et al., *Salmonella Acquires Lysosome-associated Membrane Protein 1 (LAMP1) on Phagosomes from Golgi via SipC Protein-mediated Recruitment of Host Syntaxin6.* J Biol Chem, 2012. **287**(8): p. 5574-87.
49. Steele-Mortimer, O., et al., *The invasion-associated type III secretion system of Salmonella enterica serovar Typhimurium is necessary for intracellular proliferation and vacuole biogenesis in epithelial cells.* Cell Microbiol, 2002. **4**(1): p. 43-54.
50. Patel, J.C., et al., *Diversification of a Salmonella virulence protein function by ubiquitin-dependent differential localization.* Cell, 2009. **137**(2): p. 283-94.
51. Hernandez, L.D., et al., *Salmonella modulates vesicular traffic by altering phosphoinositide metabolism.* Science, 2004. **304**(5678): p. 1805-7.
52. Hoiseth, S.K. and B.A. Stocker, *Aromatic-dependent Salmonella typhimurium are non-virulent and effective as live vaccines.* Nature, 1981. **291**(5812): p. 238-9.
53. Obert, S., et al., *The adenovirus E4-6/7 protein transactivates the E2 promoter by inducing dimerization of a heteromeric E2F complex.* Mol Cell Biol, 1994. **14**(2): p. 1333-46.
54. Grant, S.G., et al., *Differential plasmid rescue from transgenic mouse DNAs into Escherichia coli methylation-restriction mutants.* Proc Natl Acad Sci U S A, 1990. **87**(12): p. 4645-9.
55. Stecher, B., et al., *Flagella and chemotaxis are required for efficient induction of Salmonella enterica serovar Typhimurium colitis in streptomycin-pretreated mice.* Infect Immun, 2004. **72**(7): p. 4138-50.
56. Schlumberger, M.C., et al., *Amino acids of the bacterial toxin SopE involved in G nucleotide exchange on Cdc42.* J Biol Chem, 2003. **278**(29): p. 27149-59.
57. Rashidbaigi, A., H.F. Kung, and S. Pestka, *Characterization of receptors for immune interferon in U937 cells with 32P-labeled human recombinant immune interferon.* J Biol Chem, 1985. **260**(14): p. 8514-9.
58. Schlumberger, M.C., et al., *Real-time imaging of type III secretion: Salmonella SipA injection into host cells.* Proc Natl Acad Sci U S A, 2005. **102**(35): p. 12548-53.
59. Loening, A. *Site Directed Mutagenesis Protocol*. 2005; Available from: http://www.stanford.edu/~loening/protocols/Site_Directed_Mutagenesis.pdf.
60. Bryksin, A.V. and I. Matsumura, *Overlap extension PCR cloning: a simple and reliable way to create recombinant plasmids.* Biotechniques, 2010. **48**(6): p. 463-5.

61. Huang, X.a.M., W., *LALIGN finds the best local alignments between two sequences.* Adv. Appl. Math., 1991. **12**: p. 373-381.
62. Yang, Y., et al., *Inhibitors of ubiquitin-activating enzyme (E1), a new class of potential cancer therapeutics.* Cancer Res, 2007. **67**(19): p. 9472-81.
63. Henneman, L., et al., *Compromized geranylgeranylation of RhoA and Rac1 in mevalonate kinase deficiency.* J Inherit Metab Dis, 2010. **33**(5): p. 625-32.
64. Al-Quadan, T., et al., *Anchoring of bacterial effectors to host membranes through host-mediated lipidation by prenylation: a common paradigm.* Trends Microbiol, 2011. **19**(12): p. 573-9.
65. Mejia, E., J.B. Bliska, and G.I. Viboud, *Yersinia controls type III effector delivery into host cells by modulating Rho activity.* PLoS Pathog, 2008. **4**(1): p. e3.
66. Spicer, A.B. and D.F. Spooner, *The inhibition of growth of Escherichia coli spheroplasts by antibacterial agents.* J Gen Microbiol, 1974. **80**(1): p. 37-50.